Author/s:
King, AD;Hudson, D;Lim, EP;Marshall, AG;Hendon, HH;Lane, TP;Alves, O

Title:
Sub-seasonal to seasonal prediction of rainfall extremes in Australia

Date:
2020-07-01

Citation:
King, A. D., Hudson, D., Lim, E. P., Marshall, A. G., Hendon, H. H., Lane, T. P. & Alves, O. (2020). Sub-seasonal to seasonal prediction of rainfall extremes in Australia. Quarterly Journal of the Royal Meteorological Society, 146 (730), pp.2228-2249. https://doi.org/10.1002/qj.3789.

Persistent Link:
https://hdl.handle.net/11343/275618

Quarterly Journal of the Royal Meteorological Society
A journal of the atmospheric sciences and physical oceanography
RMetS

Sub-seasonal to seasonal prediction of rainfall extremes in Australia

Journal:	*QJRMS*
Manuscript ID	QJ-19-0260.R2
Wiley - Manuscript type:	Research Article
Date Submitted by the Author:	10-Mar-2020
Complete List of Authors:	King, Andrew; University of Melbourne Faculty of Science, School of Earth Sciences Hudson, Debbie; Australian Bureau of Meteorology Lim, Eun-Pa; Australian Bureau of Meteorology Marshall, Andrew; Bureau of Meteorology , Science To Services Hendon, Harry; Bureau of Meteorology, Research and Development Lane, Todd; The University of Melbourne, School of Earth Sciences Alves, Oscar; Australian Bureau of Meteorology
Keywords:	Australia, Seasonal prediction < 6. Application/context, Rainfall extremes, ACCESS-S, ENSO, IOD
Country Keywords:	Australia

Sub-seasonal to seasonal prediction of rainfall extremes in Australia

Andrew D. King[1], Debra Hudson[2], Eun-Pa Lim[2], Andrew G. Marshall[3], Harry H. Hendon[2], Todd P. Lane[1], and Oscar Alves[2]

1. School of Earth Sciences and ARC Centre of Excellence for Climate Extremes, University of Melbourne, Melbourne, Victoria, Australia.
2. Bureau of Meteorology, Melbourne, Victoria, Australia.
3. Bureau of Meteorology, Hobart, Tasmania, Australia.

Corresponding Author: Andrew D. King (andrew.king@unimelb.edu.au)

Abstract

Seasonal climate prediction to date has largely focussed on probabilistic forecasts for above- and below-average conditions in climate means. Here, we examine the possibility of making sub-seasonal to seasonal outlooks for daily-scale precipitation extremes in Australia. We first use observational data to show that significant relationships exist between climate modes, such as the El Niño-Southern Oscillation, and indices representing rainfall extremes across much of Australia. The strong observed teleconnections between climate modes and daily rainfall extremes suggest the potential for predictability on seasonal scales. The current Australian Bureau of Meteorology seasonal prediction system (ACCESS-S1) is examined for performance in predicting rainfall extreme indices using a range of measures. Ensemble hindcasts, consisting of 11 members initialised every month during 1990-2012, perform well for some extreme rainfall indices on short lead-times (up to one month). We note that at short lead-times forecasts are aided by skilful weather prediction, so forecast performance drops at lead-times of a week or more. Forecast performance is lower in austral summer than other seasons and greater in the north and interior of the continent, particularly in the dry season, than elsewhere. The ACCESS-S1 ensemble is over-confident but exhibits some reliability in probabilistic forecasts of above- or below-average number of wet days and intensity of the highest daily maximum precipitation, especially in northern Australia. ACCESS-S1 captures the broad pattern of relationships between climate modes and rainfall extremes that are observed. For two case studies of unusually extreme precipitation, ACCESS-S exhibits contrasting performance for forecasts of extreme rainfall anomalies beyond the first month. These results suggest that ACCESS-S1 may be used to produce outlooks for some rainfall indices, such as the number of wet days and the intensity of the wettest day, for the month ahead.

Keywords: Australia, Seasonal Prediction, Rainfall Extremes, ACCESS-S, ENSO, IOD

1. Introduction

Australia has a highly variable climate especially for rainfall (Nicholls *et al* 1997) with droughts and extreme rainfall events that have large economic, social, and environmental impacts. The highly variable climate of Australia is, in large part, due to its position between the Indian and Pacific Oceans with much of the variability in rainfall linked to the Indian Ocean Dipole (IOD) and El Niño-Southern Oscillation (ENSO) in addition to other climate modes, such as the Southern Annular Mode (SAM) and the Madden-Julian Oscillation (MJO) (e.g. Risbey *et al* 2009).

It is not only mean rainfall that has strong relationships with these climate modes but also rainfall extremes (Min *et al* 2013, King *et al* 2014). For example, there are significant correlations between the Niño-3.4 index and seasonal maximum 1-day precipitation (Rx1day) totals in austral winter and spring across much of northern and eastern Australia (Min *et al* 2013). Similarly strong relationships between the Dipole Mode Index, representing the IOD, and Rx1day in southern Australia in austral winter and spring, and between the SAM index and Rx1day in the southeast of Australia in austral spring and summer were observed (Min *et al* 2013). While patterns of extreme rainfall indices are more spatially inhomogeneous than for mean rainfall, for Rx1day and the maximum consecutive 5-day rainfall totals (Rx5day) there are significant relationships with ENSO and the IOD (King *et al* 2014).

The strong teleconnections between slowly-evolving climate modes and Australian climate variability lend themselves to seasonal predictability. Australia has a long history of seasonal prediction (Quayle 1929, Nicholls and Woodcock 1981, Nicholls 1985). It was recognised long ago that given a particular state of a climate mode is in place, for example La Niña, the slow evolution of the climate mode would mean that an increased likelihood of climate anomalies in one direction would often persist for several months. As a result, the Australian

Bureau of Meteorology (BoM) made empirical seasonal predictions from 1989 based on observed teleconnections between ENSO and Australian climate variability (McBride and Nicholls 1983, Nicholls 1983, 1979) and subsequently the Indian Ocean teleconnection (Drosdowsky and Chambers 2000, Stone *et al* 1996). The BoM developed and operationalised dynamical prediction models in the early 21st century (Alves *et al* 2003, Cottrill *et al* 2013) and the current operational system, the Australian Community Climate and Earth-System Seasonal model (ACCESS-S1; Hudson *et al* 2017), is now used to make probabilistic seasonal outlooks for sea surface temperatures (SSTs), ENSO, the IOD and also Australian climate (including monthly- and seasonal-average precipitation and maximum and minimum temperatures).

Given that the strong teleconnections between climate modes and Australian rainfall variability have been shown to extend to rainfall extremes, the possibility of seasonal prediction of rainfall extremes should be considered. Large-scale or persistent rainfall extremes have substantial impacts as they often result in catastrophic flooding. This was the case during the austral summer of 2010/11 when heavy rainfall led to severe floods across much of Queensland resulting in multiple fatalities and large economic losses of several billion dollars (Australian Business Roundtable for Disaster Resilience & Safer Communities 2016). Accurate seasonal prediction of not only the mean precipitation for the month or season, but for precipitation extremes as well, has the potential to have large economic benefits to the agricultural sector and other industries (The Centre for International Economics 2014a, 2014b).

In this study we revisit the observed teleconnections between climate modes and different indices for rainfall extremes. Based on the observational analysis we select suitable indices where seasonal prediction may be possible and we subsequently investigate model performance in prediction of these indices in the ACCESS-S1 hindcasts. We use a range of

verification statistics to assess forecast performance in ACCESS-S1 at a range of lead-times and we examine the model representation of relationships between climate modes and rainfall indices.

The remainder of the paper is organised as follows: in section 2 we discuss the datasets used and the methods applied in our analysis, in section 3 we motivate our ACCESS-S1 analysis using observed relationships between climate modes and rainfall extremes, in section 4 we examine the performance of ACCESS-S1 using a range of verification metrics, in section 5 we analyse ACCESS-S1 relationships between climate modes and rainfall extremes, in section 6 we focus on two case studies, and in section 7 we discuss and conclude our analysis.

2. Data and Methods

2.1. Observational datasets

For verification of the forecasts, a gridded rainfall product was deemed most suitable for comparison. Daily rainfall data from the Australian Water Availability Project (AWAP; Jones *et al* 2009) for 1900-2017 were extracted on a regular 0.05° grid. The AWAP rainfall product is derived from interpolating all available *in situ* rainfall observations onto a grid using a splining technique (more details can be found in Jones *et al* 2009). Although there are issues with AWAP underestimation of rainfall extremes, in regions where station data that AWAP is derived from are dense the variability in mean and extreme rainfall is captured well (King *et al* 2013b). In regions where stations are sparse, the AWAP product performs less well, thus a mask was applied over central Australia (selected as the region with no data coverage prior to 1930) and the region is not analysed further. The AWAP data were interpolated onto a regular 0.25° grid for all subsequent analysis.

A selection of mean and extreme rainfall indices was investigated for their relationships with climate modes (Table 1). The five extreme rainfall indices (in addition to total rainfall: PRCPTOT, sometimes also referred to as mean rainfall here) are adapted from those recommended by the Expert Team on Climate Change Detection and Indices (ETCCDI; Zhang *et al* 2011) and are chosen to represent different characteristics of extreme rainfall (Haylock and Nicholls 2000) for which relationships with climate modes and seasonal predictive skill may be assessed. There are intensity-based indices, including Rx1day, frequency-based metrics, including the number of wet days (WD), and a contribution-based index, the proportion of monthly rainfall due to the wettest day (Rx1C). These indices were calculated using the AWAP dataset for 1900-2017 in each calendar month to allow the relationships between climate modes and rainfall indices to be robustly established. Two indices (R90P and R90PTot) use a climatological 90th percentile which is derived for each calendar month separately and excludes non-rain days in its calculation (otherwise in many cases the 90th percentile would be zero). Note, while the WD index is classified as an ETCCDI extreme rainfall index it is relevant to the whole statistical distribution of rainfall not just the tail. While the WD index is not a truly extreme index it does represent a useful alternative characteristic of rainfall to PRCPTOT.

To examine observed extreme rainfall relationships with coupled ocean-atmosphere climate modes, a dataset of observed SSTs was used. The Met Office Hadley Centre Sea Ice and Sea Surface Temperature product was analysed (HadISST; Rayner *et al* 2003). The monthly SST data were used to compute the Niño-3.4 index to represent ENSO [170°W-120°W, 5°S-5°N], the Dipole Mode Index to represent the IOD [Western pole: 50°E-70°E, 10°S-10°N, Eastern pole: 90°E-110°E, 10°S-0°N] (Saji *et al* 1999), and the North Australian SST index [110°E-150°E, 15°S-0°N] (Nicholls 1984, Catto *et al* 2012). Area-average SSTs were computed for the relevant regions and the climate mode indices were computed by detrending the data in

each calendar month individually by subtracting a 31-year moving average. In the case of the DMI, the detrending was performed before the difference between the western and eastern poles was computed, but the sensitivity to this choice is minimal.

The relationships between climate modes and different extreme rainfall indices were assessed through computing Spearman rank correlation coefficients, to account for non-normal distributions of extreme indices across most of Australia in most months. The areas of Australia (excluding the masked region of central Australia) where these correlations are significant at the 5% level were aggregated for summarising the relationships between the climate modes and each rainfall index.

2.2. The ACCESS-S1 hindcasts

ACCESS-S1 is a state-of-the-art seasonal prediction model system used operationally by the BoM (Hudson *et al* 2017). The current version of the model is the same as the UK Met Office model GloSea5-GC2 (MacLachlan *et al* 2015) but the ensemble generation scheme, ensemble size and the configuration of the system for operational forecasting differ (see Hudson *et al* 2017 for further details). The ACCESS-S1 hindcasts have been used previously to evaluate the model for its skill in temperature and precipitation totals over Australia (Hudson *et al* 2017), the evolution of ENSO, the IOD and MJO (Hudson *et al* 2017, Marshall and Hendon 2019), skill for SST (de Burgh-Day *et al* 2019, Smith and Spillman 2019), and tropical cyclone frequency and location (Camp *et al* 2018). Here we analyse ACCESS-S1 performance in prediction of extreme precipitation indices.

The hindcasts used in this analysis cover the 1990-2012 period with 11-member ensembles initialised four times per month each running for seven months. For this analysis, we primarily used the hindcasts initialised on the 1st of each month and calculated each rainfall index for each calendar month and ensemble member at lead-0, lead-1 month, and lead 2-

168 months (e.g. for forecast verification in March 1990, leads-0, 1 and 2 correspond to runs
169 starting 1st March 1990, 1st February 1990, and 1st January 1990, respectively).

170 We used the ACCESS-S1 hindcasts that have been calibrated to AWAP daily rainfall using a
171 quantile-matching method applied to daily precipitation in 11-day windows (Bureau of
172 Meteorology 2019). The calibrated data are on the same regular 0.05° grid as AWAP and for
173 this study were interpolated to the same regular 0.25° grid as was applied to AWAP. The
174 high resolution 0.05° data are not required for the verification of seasonal forecasts across the
175 entire continent, so regridding was performed to a coarser resolution to reduce computational
176 costs. The resolution dependence of the results was tested using a coarser grid, at a lower
177 resolution than the raw model output, and it was found to not have a large effect (not shown).
178 Despite the calibration of ACCESS-S1 hindcasts to AWAP, there are still differences
179 between ACCESS-S1 hindcasts and AWAP over the common 1990-2012 period in the
180 average values of each extreme rainfall index (see Figure S1 for an example based on
181 Rx1day). As a result the ACCESS-S1 anomalies were calculated relative to ACCESS-S1
182 rather than AWAP as discussed further in Section 2.3.

183 **2.3. Anomaly calculation and forecast verification statistics**

184 The rainfall indices were evaluated in ACCESS-S1 relative to AWAP in anomaly space. In
185 AWAP the anomalies for each rainfall index in each calendar month were calculated relative
186 to all other years in the same calendar month at the same location. For example, Rx1day in
187 January 2000 was calculated as an anomaly from the median of all other January Rx1day
188 values in the 1990-2012 period excluding January 2000 itself (i.e. cross-validation). The
189 median was used as in many cases the statistical distributions of extreme rainfall indices are
190 strongly positively skewed.

As the ACCESS-S1 model has biases compared to AWAP, the model itself was used to construct climatologies. The same principle of computing the index anomaly from all equivalent values was applied (same location, calendar month, and for ACCESS-S1, the same lead time also). The climatology is also composed of all 11 ensemble members. For example, Rx1day in January 2000 at lead-0 in ACCESS-S1 ensemble member 5 was calculated as an anomaly relative to the median of all other January Rx1day values in ACCESS-S1 at lead-0 for 1990-2012 using all ensemble members but excluding January 2000 itself. All subsequent analysis of ACCESS-S1 was performed in anomaly space. Also, while performance analysis of ACCESS-S1 could be undertaken for different points in the distribution (e.g. upper or lower terciles or deciles), we focus much of our analysis on performance in forecasting above-median conditions. This is in part because this is the primary mode of delivery for the BoM seasonal outlooks and also because the verification statistics tend to be more robust where sample sizes are larger (e.g. Wilks 2010).

There are a plethora of metrics that may be used in assessing seasonal prediction verification with different measures designed to represent different aspects of forecast performance (e.g. Wilks 2011, Vitart *et al* 2019). A selection of metrics designed to examine different aspects of the performance of the ACCESS-S1 hindcast ensemble in predicting rainfall extremes were used here. Most of these metrics are displayed using maps or aggregated data across Australia with adaptations to these metrics designed to account for non-Gaussian distributions of the extreme indices and greater ease in the visualisation and interpretation of results.

Firstly, mapped Spearman-rank correlation coefficients were computed between ensemble median ACCESS-S1 values and AWAP values for each calendar month and each index at lead-0 and lead-1. The correlation coefficients allow for the temporal variations of the indices between the observational product and the model to be compared. To condense this

information for easier comparison between indices, the Australia- and state-average correlation coefficients were calculated for all indices and calendar months. These are Pearson correlations as the Fisher Z-transform was used to calculate area-average values and compute associated correlation coefficients. Matrices of these Australia- and state-average correlation coefficients allow for visual comparison of this measure of model performance between states, indices and calendar months. The Australia-average correlation statistics were also calculated using the other initialisation dates within each month (9th, 17th and 25th) to examine the performance of ACCESS-S at more lead-times. These were also calculated for all indices and calendar months using the Fisher Z-transform technique.

The proportion correct (PC) was also employed as a metric to assess the fraction of instances where ACCESS-S1 was correct in a seasonal prediction. This was applied to each index by examining the proportion of instances where the ACCESS-S1 ensemble median anomaly was of the same sign as the AWAP anomaly.

The Brier Skill Score (BSS) was calculated to examine how skilful the ACCESS-S1 hindcast simulations are relative to climatology. This was also applied to all indices and all locations across Australia in each calendar month using probabilistic forecasts calculated using the ACCESS-S1 ensemble and comparing to AWAP. The BSS was computed for forecasts of the probability of above-average values of each index.

Rank histograms show if an ensemble of forecasts appropriately samples forecast uncertainty by comparing observations with the range of the ensemble member forecasts (Wilks 2011). Goodness of ensemble forecasts is indicated by even distribution of the frequency of observations in all ranks of ensemble forecasts. Rank histograms were used to examine whether ACCESS-S1 is over- or under-confident in the ensemble spread for different indices and locations. The most frequent rank of AWAP relative to the ACCESS-S1 ensembles was

plotted to produce maps and warm season months (defined as November to April) and cool season months (May-October) were aggregated to increase sample size for compiling the rank histograms. In addition to these maps, box-plots displaying the frequency of observation in each rank for all locations across Australia were constructed. An estimate of the 95% confidence interval on the frequency of ranks that could be expected by chance was made. This was computed by 138 random draws from a uniform distribution of 12 values. The 138 draws from this distribution matches the number used in forming the rank histograms which are each based on six values (for the six months in the warm and cool seasons) over a 23-year hindcast. This process was repeated 10000 times and for a random rank the 2.5th and 97.5th percentiles of frequency were estimated. Values outside of this range are deemed to be unlikely to occur due to chance.

The reliability of the ACCESS-S1 probabilistic forecasts was computed by binning the forecast probabilities into 11 categories spanning from a probability of 0% to 100%, and computing the corresponding observed probability of the event for those forecasts. Reliability is plotted on a reliability diagram, but here we also use maps to represent reliability in indices at individual locations across Australia. As for the rank histograms, reliability was computed on composites of warm season and cool season months rather than individual calendar months to generate a larger sample size.

2.4. Further ACCESS-S1 evaluation

In addition to the metrics described above, the relationship between climate modes and rainfall indices in ACCESS-S1 was compared with observed relationships. For the calendar months with the largest areal signature of statistically significant ($p<0.05$) observed correlations between each climate mode and total precipitation (as listed in Table 2 and extracted from Figure 1), the observed and simulated relationships were compared. For SAM,

the relationship with rainfall means and extremes is strongest in late spring and early summer (Hendon *et al* 2014, Lim and Hendon 2015, Min *et al* 2013), so November was chosen.

The relationships between climate modes and rainfall means and extremes in ACCESS-S1 were investigated in two different ways. Firstly, using the calendar months with the strongest observed relationships between each of the four climate modes and mean rainfall, the regression coefficient of each rainfall index onto each climate mode over 1990-2012 was computed for each location across Australia using both observed climate modes and rainfall indices, and ACCESS-S1 ensemble-mean simulated climate modes (at leadtime-0 months) and rainfall indices. This allows the observed and simulated teleconnections to be compared directly.

Secondly, the five years where each of the calendar months that ENSO, the IOD, N. Australian SSTs and the SAM were in their most positive and negative phase based on the observational data during the 1990-2012 hindcast period were composited (Table 2). The median difference (to limit sensitivity to outliers) between rainfall indices in the positive and negative phases of each index was computed for each of AWAP and ACCESS-S1. The Spearman rank pattern correlation coefficient was computed between AWAP and ACCESS-S1 to allow for a quantitative measure of model performance in the patterns of the mean and extreme rainfall anomalies associated with each climate mode. This analysis allows ACCESS-S1 to be compared with observations for specific periods of strong climate mode phases. This provides a test of performance in prediction of climate mode-extreme rainfall relationships.

In addition, during the hindcast period of 1990-2012 there were several occasions where impactful large-scale extreme rainfall events occurred. The ability of ACCESS-S1 to predict anomalies of mean and extreme precipitation in the case of two such events was examined.

The two events investigated in more detail were December 2010, when extreme rainfall resulted in severe flooding across large areas of Queensland (van den Honert and McAneney 2011), and June 2007, when flooding occurred in several areas of Australia some of which was associated with an East Coast Low system affecting New South Wales (Mills *et al* 2010). The anomalies in ACCESS-S1 mean and extreme precipitation indices at lead-0, lead-1 months and lead-2 months were compared with the observed anomalies. Again, Spearman rank pattern correlation coefficients between AWAP and ACCESS-S1 were computed. The correlation coefficients were computed between each ACCESS-S1 ensemble member and AWAP.

3. Observed relationships between climate modes and extreme rainfall indices

The observed relationships between ENSO, IOD and N. Australian SSTs, and rainfall indices were examined by correlating representative indices for these climate modes with rainfall indices (Table 1). The relationships between these climate modes and rainfall means and extremes are strongest in different areas and seasons (Risbey *et al* 2009, Min *et al* 2013, King *et al* 2014). To condense this information, Figure 1a-c shows bar plots of the area of Australia for which there are significant correlations ($p<0.05$) between indices representing ENSO, IOD and N. Australian SSTs and each rainfall index, respectively. The strongest relationships between these climate modes and rainfall indices tend to be in austral winter and spring with the area under significant correlation peaking earliest for N. Australian SSTs (in around July), then peaking for the IOD in September and ENSO in October. In general, the bar plots indicate stronger relationships between the climate modes and mean rainfall than for extreme rainfall indices (Min *et al* 2013, King *et al* 2014), but there is a large difference in results between some of the extreme rainfall indices. In particular, the contribution metric used here, Rx1C, shows much weaker relationships with all the climate modes than the other indices exhibit.

The area of Australia that exhibits a significant relationship between rainfall indices and any of ENSO, the IOD and N. Australian SSTs for a given calendar month was aggregated as this gives an indication of the potential for predictability more generally (Figure 1d). Unsurprisingly, given the results shown in Figure 1a-c, austral winter and spring are the times of year when Australian mean and extreme rainfall indices exhibit more widespread significant relationships with climate modes. There are months where WD has more widespread relationships with climate modes than are observed for mean rainfall, but the Rx1C index exhibits substantially weaker relationships than the other indices. Based on this observational analysis we examine the predictive skill of these extreme rainfall indices in ACCESS-S1 (aside from Rx1C).

4. Performance of extreme rainfall prediction in ACCESS-S1

Performance in ACCESS-S1 predictions was first assessed using the Spearman's rank correlation coefficient based on the ensemble-median of the hindcast set and AWAP for lead-0. These are shown for each calendar month for Rx1day in Figure 2 and, for most of Australia and in most calendar months, the correlations are positive and often significant. There is a general pattern towards higher correlations in the interior of the continent and for the weaker correlations to be in late spring and early summer months. Unfortunately, the performance of ACCESS-S1 is better during drier times in the year when the Rx1day totals tend to be lower (Figure S2).

To condense the information from these correlation maps, correlation coefficient matrices were produced using all indices for Australia-average values and for each state and territory of Australia at lead-0 (Figure 3). Note, these are Pearson correlation coefficients due to the averaging applied to Z-scores to conserve normality. The distinct seasonal cycle in forecast performance, as measured by correlation coefficients, is apparent in most of the mainland

states and territories, but there are different levels of performance between indices. Aside from mean precipitation, the WD index also exhibits stronger correlations than are seen for the other indices. The R90PTot index shows generally weak skill with the R90P and R10mm indices also performing relatively poorly in line with the weaker climate mode relationships found for these indices (Figure 1). The general pattern of greater forecast performance in the north and east is also clear with ACCESS-S1 performing better, using the correlation coefficient measure, in Queensland and the Northern Territory than elsewhere.

A similar plot for lead 1-month correlations was also produced (Figure 4). These longer lead forecasts exhibit far poorer model performance than the lead-0 forecasts. Overall, in many cases, correlation coefficients are still positive but few are statistically significant. While all the correlations are relatively weak at this lead-time they are still higher in northern Australia, albeit at a drier time of year, and for PRCPTOT and WD than for other indices.

The effect of lead-time on model performance was investigated using ACCESS-S1 simulations initialised at other times within the month as well as the 1st of the month simulations. Figure 5 shows the Australian-average correlations between ACCESS-S and AWAP for a) Rx1day and b) PRCPTOT in each calendar month using simulations initialised on 9th, 17th and 25th in the months prior to the month of interest. The performance of ACCESS-S decreases even at lead-times of around one week or half a month with a tendency for greater reduction in model performance with lead-time during the warm season months than in the cool season. The remaining analysis is based on the 1st of the month simulations only.

The proportion correct (PC) was computed comparing the sign of the ACCESS-S1 ensemble median anomaly with the sign of the observed anomaly (Rx1day at lead-0; Figure S3). The PC results largely mirror those found using the correlation coefficients with PC falling below

0.5 (i.e. negative skill compared to a climatological forecast) in some areas of Australia in late spring and early summer, but generally higher in other seasons. The PC metric performs poorly where the median value is at or near zero (i.e. no heavy rainfall has occurred), which is true for several indices considered here, especially in northern Australia in the dry season. Australia- and state-average values of PC (not shown) are less useful than the correlation coefficient equivalent values (Figure 3) due to the high frequency of zero-values and skewness in statistical distributions for many indices. For forecasts of the probability of above average conditions, we use the Brier Skill Score (BSS) computed relative to a climatological forecast. The BSS shows skill above climatology over most of Australia in most months for PRCPTOT and some extreme indices (see Figure S4 for an example for Rx1day at lead-0). Once again, December shows substantially less skill than is found in other calendar months. Skill, as measured by the BSS, is above climatology in most of northern Australia and in most months outside late spring and early summer.

To better understand the characteristics of the ACCESS-S1 ensemble, we used rank histograms comparing the frequency of AWAP ranks relative to different points within the ACCESS-S1 ensemble. Over most of Australia, AWAP monthly rainfall totals and Rx1day tend to be too frequently outside of the lowest rank of the ensemble, indicating that ACCESS-S1 ensemble has a wet bias (Figure S5). In contrast, AWAP WD anomalies are too frequently outside of the highest rank of the ensemble, indicating that the number of wet days are systematically underpredicted by ACCESS-S1. Aggregating across Australia we observed that for PRCPTOT and Rx1day in most places the observed anomalies are below the entire ACCESS-S1 ensemble considerably more than could be expected by chance (as evidenced by the frequency in the lowest rank outside of the grey area in Figure 6). The ACCESS-S1 ensemble is under-dispersive for PRCPTOT, Rx1day, and WD in both the warm season and cool season as implied by the rank histogram tending to be U-shaped because the ensemble

386 members tend to be too similar and biased against the verification. The ACCESS-S1
387 ensemble is more dispersive for WD than other indices, but this may be in part due to the
388 discrete values this index can take even in anomaly space when the climatological value is a
389 median rather than a mean.

390 The reliability of probabilistic forecasts relates to how well the predicted probabilities of an
391 event correspond to their observed frequencies and, like the rank histogram, can provide an
392 indication of forecasting bias. The reliability of lead-0 Rx1day forecasts in the warm season
393 (Figure 7) and cool season (Figure S6) is visualised first through maps of the observed
394 frequency of above-average anomalies given different fractions of the ACCESS-S1 ensemble
395 are above average. The maps illustrate that as an increasing fraction of the ACCESS-S1
396 ensemble is above average, there is a higher observed frequency of above-average values.
397 There is a great deal of noise between locations in this pattern such that reliability diagrams
398 based on single locations and with relatively low sample size would not be informative. To
399 account for this issue, the reliability was also plotted on traditional reliability diagrams,
400 aggregating values from across Australia to produce box plots (Figure 8). These show that the
401 forecasts for PRCPTOT, Rx1day and WD are over-confident (i.e. under-dispersed), e.g.
402 probabilistic forecasts of under 10% chance of above-average conditions are commonly
403 associated with observed frequencies of above-average conditions around 20%, and, at the
404 upper end of the scale, forecasts of above 90% chance of above average conditions are
405 commonly associated with observed frequencies of above-average conditions around 80%.
406 Despite the overconfidence in the forecasts, the majority of the distributions displayed
407 through box plots are in the dark grey region indicating there is some skill over a
408 climatological forecast. Overall, the reliability diagrams suggest slightly greater skill and
409 reliability over more of Australia in the PRCPTOT and WD forecasts than the Rx1day
410 forecasts. The reliability diagrams were also plotted for northern and southern Australia,

411 defined as areas north and south of 26°S respectively (Figures S7, S8). These point to a
412 greater degree of over-confidence in the ACCESS-S1 ensemble aggregating across southern
413 Australia compared with northern Australia in both the warm and cool seasons. This regional
414 difference in ACCESS-S1 ensemble performance is also suggested by the mapped reliability
415 plots (Figures 7, S6).

416 **5. Relationships to climate modes**

417 The slow evolution of climate modes and their strong teleconnections to Australian climate
418 give rise to high potential predictability for the continent. As such it is vital that the
419 relationship between climate modes, such as ENSO, and Australian rainfall indices are well
420 represented for there to be confidence that ACCESS-S1 may be useful for the sub-seasonal to
421 seasonal prediction of rainfall indices. It has been shown previously that ACCESS-S1
422 exhibits skill in multi-week to seasonal forecasts of ENSO, IOD and SAM (Hudson *et al*
423 2017), so accurate representation of teleconnections to Australian climate should aid skill in
424 prediction of rainfall indices.

425 To investigate how Australian rainfall indices are associated with climate modes, the calendar
426 months with the largest areal extent of significant correlations between ENSO, the IOD and
427 N. Australian SSTs and mean rainfall were selected (Figure 1; Table 2). The observed and
428 simulated teleconnections between these climate modes and the rainfall indices were
429 compared by regressing each observed and simulated (model lead-0) rainfall index onto the
430 corresponding observed and simulated climate mode indices (Figure 9). Note, the use of the
431 ACCESS-S1 ensemble mean climate mode slightly reduces the amplitude of regression
432 coefficients relative to the observed climate modes. The regression maps are similar between
433 AWAP and ACCESS-S1 with the model capturing the broad relationships in the observed
434 data across the mean and extreme rainfall indices and the different climate modes. The

observed ENSO relationships with all three extreme indices shown here are stronger than in ACCESS-S1 over most of northern and eastern Australia. The observed IOD relationship with mean and extreme rain indices tends to be stronger in the south of Australia but in the model the teleconnection may be shifted slightly (this is seen most clearly in Figure 9s,t). There is more spatial inhomogeneity in the observed regression maps than in ACCESS-S1 as an ensemble-mean is used in the model.

To examine how the ACCESS-S1 model performs when the climate modes are in strongly positive or negative phases another test was performed. The five years with the most extreme values of each climate mode in each direction, using the observational data only, were selected and used to produce composite median differences in the rainfall indices in both AWAP and ACCESS-S1. For example, in AWAP, La Niña Octobers are wetter on average than El Niño Octobers across most of the continent and ACCESS-S1 reproduces this pattern well (Figure 10a,b). This tendency for wetter conditions in La Niña phases also holds true for Rx1day and WD and ACCESS-S1 captures the corresponding patterns well also (Figure 10i,j,q,r). The differences in mean and extreme rainfall indices between cases of positive and negative IOD and positive and negative N. Australian SST extremes are also captured in general in ACCESS-S1 (Figure 9). The SAM also exhibits a strong teleconnection to Australian rainfall (Lim and Hendon 2015, Risbey *et al* 2009, Min *et al* 2013) so a good representation of this relationship in ACCESS-S1 is important especially in southern Australia and on the east coast. The SAM is noisier than the other climate modes and the observed differences in mean and extreme precipitation between SAM phases in November show less of a clear pattern than for ENSO, the IOD, or N. Australian SSTs in their selected months. Nonetheless, ACCESS-S1 broadly captures the expected pattern of reduced mean rainfall, less intense extreme rain days, and fewer wet days in eastern Australia in negative SAM relative to positive SAM phase.

6. Case study analyses: December 2010 and June 2007

It is of particular importance that ahead of periods of extreme weather, seasonal predictions are accurate enough to allow for planning well ahead of time to mitigate the risks associated with these events. One warm season and one cool season case study of particularly extreme rainfall events were investigated in more detail. Firstly the month of December 2010 which saw record-breaking rains and extreme flooding in Queensland especially (van den Honert and McAneney 2011) was selected. This event occurred during a strong La Niña, which are typically associated with very wet conditions in the northeast of Australia (Risbey *et al* 2009, Klingaman *et al* 2013), and very high local SSTs also increased the precipitation totals during this event (Evans and Boyer-Souchet 2012). The observed PRCPTOT, Rx1day, and WD anomalies illustrate the wetter-than-average conditions across all these indices during December 2010 (Figure 11d,h,l). At lead-0 (i.e. 1st December 2010 simulations), the ACCESS-S1 ensemble median anomalies show a very similar pattern to the observed anomalies. The pattern correlations at this lead-time with the observed anomalies are high, except in Rx1day, but this is principally due to the higher spatial inhomogeneity in that index. At longer lead-times of lead-1 month (1st November 2010) and, to a lesser extent, lead 2-months (1st October 2010) there is still an indication of wetter conditions likely in December 2010, but the signal is less clear and the pattern of very wet conditions observed in southeast Queensland and eastern New South Wales is not forecast. As seasonal forecasts are usually communicated in probabilistic terms, it is promising that a majority of ensemble members forecast wetter-than-normal conditions across the rainfall indices for much of Australia even at one-to-two-month lead-times. Given that December is the calendar month in which ACCESS-S1 appears to have the worst performance based on the previous results (e.g. Figure 2), it is also promising that for a particularly extreme event as occurred in December 2010,

there is some evidence of ACCESS-S1 providing useful forecasts in unusually extreme circumstances.

The other case study examined was June 2007 when an East Coast Low brought extreme rainfall to coastal New South Wales (Mills *et al* 2010). While the north and east of Australia were unusually wet, most of the south including Tasmania was drier than normal (Figure 12) as high pressure systems were located over the Great Australian Bight for much of the month. The lead-0 forecasts (from 1st June 2007) performed well in capturing the pattern of very wet anomalies in the east and the dry conditions in the south. At longer lead-times (simulations initialised on 1st April 2007 and 1st May 2007) the ACCESS-S1 forecasts performed considerably less well in capturing the extreme wet anomalies in the east, although the drier anomalies in the south are better predicted.

7. Discussion and conclusions

In this study we have sought to assess forecast performance in seasonal outlooks of precipitation extremes in Australia using ACCESS-S1, the current BoM seasonal prediction system. We firstly illustrated that there is a strong potential for predicting some rainfall extremes indices due to the strong teleconnections that exist with climate modes, such as ENSO. Using a range of different measures we have found that ACCESS-S1 exhibits a similar degree of model performance in the WD index as it does for mean precipitation. ACCESS-S1 is less skilful in predictions of extreme rainfall indices, particularly in more "extreme" extreme indices that represent rarer extremes, such as total rainfall on days above the 90th percentile. ACCESS-S1 performs reasonably well in capturing teleconnections between climate modes and rainfall indices, and in the predictability of rainfall indices during strong phases of climate modes. In our December 2010 case study, ACCESS-S1 performed well at lead-1 month.

Further analysis of ACCESS-S1 to understand model biases, ensemble overconfidence, and poor model performance in some indices is required, especially in late spring and early summer when the wet season often begins and seasonal outlooks for rainfall are especially useful. Indeed, while not a surprising result, it is disappointing that the model performs relatively poorly in populated areas of the continent where extreme rainfall can have more economically-costly impacts, so research that would lead to improved performance in future iterations of ACCESS-S around Sydney, Melbourne and other major cities would be of particular use.

Indices where ACCESS-S1 performs poorly tend to be those which are more spatially inhomogeneous and less strongly associated with variations in mean precipitation (Figure S9). In December, when ACCESS-S1 performance is particularly poor, there are relatively weak observed relationships between climate modes and Australian mean and extreme rainfall indices (Figure 1d), so it may be that without strong teleconnections, rainfall anomalies are driven by mesoscale-to-synoptic-scale processes that are more randomly driven than otherwise is the case, and thus more difficult to forecast on seasonal timescales.

The analysis of subseasonal-to-seasonal prediction in daily-scale climate extremes is an emerging field (Sillmann *et al* 2017) with few analyses to date (Lee *et al* 2017, Pepler *et al* 2015a) and some focussed solely on temperature extremes (Bhend *et al* 2017, Hudson and Marshall 2016). This is the first comprehensive analysis of sub-seasonal to seasonal prediction of daily-scale rainfall extremes in Australia. As this field is relatively new, and seasonal prediction models continue to improve such that forecasting of extremes becomes more viable, the issue of suitable model performance verification for extreme indices will become more pressing. Here, we used modified versions of common verification measures to assess performance in the ACCESS-S1 model. For instance, we constructed climatologies of median-values instead of means and produced maps of correlation coefficients between

ACCESS-S1 and our observational dataset using the non-parametric Spearman rank method instead of Pearson correlations. For some extreme indices there are performance metrics that are less useful than others. In particular, proportion correct, when applied to the sign of anomalies, is of little use for indices where the median is zero. It could also be misinterpreted for indices like the number of wet days if the climatology is a median, as there is the potential for a high proportion of predicted and observed values to be exactly average rather than above or below average. The use of a combination of metrics and careful application after some modifications was necessary. For more "extreme" indices than were considered here, which tend to be the indices that would signify rarer high-impact events, the issue of suitable model performance verification becomes even more important and sample size limitations become more of an issue. More extreme rainfall indices tend to be more spatially inhomogeneous (e.g. King *et al* 2014), so location-specific measures of model performance that perform well in mean rainfall may be of less use as the spatial pattern of an index becomes noisier. Performance measures that draw on techniques used for verification of highly localised extreme rainfall events in high-resolution numerical weather prediction models (e.g Ebert and McBride 2000, Roberts 2008) may be of use for more "extreme" extreme indices that represent only rarer events than those captured by the indices examined here.

The indices for extreme rainfall used here were based on the ETCCDI extreme rainfall indices (Zhang *et al* 2011) more commonly used for climate change detection and modelling (e.g. Sillmann *et al* 2013, Donat *et al* 2013). The analysis of ACCESS-S1 performance in these indices is useful in understanding model biases and other issues, but we have not determined the utility of these indices for seasonal prediction in conjunction with relevant stakeholder groups. Previous work has indicated that for seasonal prediction to be of greatest use to stakeholders, the predictive skill is only one factor amongst several that determine

whether seasonal outlooks will be used in decision-making processes (Ziervogel and Downing 2004, Hartmann *et al* 2002). Given the demonstrable performance in predicting some rainfall indices in ACCESS-S1, further work to determine which indices would be of use to specific stakeholder groups and how they will inform decisions is required.

The analysis we have conducted is primarily focussed on forecasts for the month ahead, but our analysis for longer lead-times suggests a substantial decrease in model performance. There may be more promising results if extremes indices are designed for the analysis of sub-seasonal prediction (Hudson *et al* 2011, Marshall *et al* 2014), such as on timescales of two-to-three or three-to-four weeks. For shorter time-windows the extremes indices would need to be redesigned to be relevant on the timescale of a week rather than a month.

It is likely that some of the model performance in the lead-0 forecasts is due to predictability on the timescale of numerical weather prediction, and this is suggested from the reduced performance in ACCESS-S1 for simulations initialised several days before the start of the month compared with 1st of the month simulations (Figure 5). If an extreme rainfall event is forecast to occur in the first seven to ten days after the runs are initialised, there is more likely to be more consistency across the ensemble in the anomalies associated with extreme rainfall indices. This effect may be part of the reason that the June 2007 prediction (Figure 12), initialised on 1st June, was particularly accurate as the East Coast Low (ECL) brought the heaviest rainfall on 7th June. In contrast, in December 2010 (Figure 11), where the lead-0 forecasts still perform well, the heaviest rainfall occurred near the end of the month in most of the northeast of Australia. More generally, the model performance of seasonal predictions of rainfall extremes is likely to be connected to the predictability of the weather systems that bring the extreme rainfall and this will vary greatly. For instance, ECLs, in common with other mesoscale systems over Australia, are not strongly related to climate modes (Pepler *et al* 2015b) and require the confluence of several important ingredients to occur (Cavicchia *et*

583 *al* 2019). It is likely that ECLs have less inherent predictability than other major rain-bearing
584 systems including tropical cyclones which have stronger relationships to climate modes such
585 as ENSO (Dowdy *et al* 2012, Kuleshov *et al* 2008). This effect likely contributes to the
586 pattern of model performance across Australia with greater model fidelity in northern areas
587 and the interior than in the south and near coasts.

588 The results of this analysis are drawn from a 23-year hindcast set of ACCESS-S1
589 simulations, and focussed on 1st of the month simulations to ensure consistency, for the 1990-
590 2012 period. This is below the 30 years that the World Meteorological Organisation would
591 use to define climatologies Thus, there is an assumption that this period and length of period
592 are sufficient in assessing the performance of ACCESS-S1. A period of 23 years is typically
593 too short to obtain statistically robust results, particularly for aspects of the prediction system
594 that are inherently noisy, such as relatively localised forecasts. In addition, a sufficiently long
595 hindcast set is necessary for including an adequate number of cases of the low frequency
596 influences on Australian climate, like the different phases of ENSO, and for knowing how
597 model performance may vary based on the state of these climate drivers. Furthermore,
598 teleconnections between climate modes and specific weather systems have been shown to be
599 variable in the past with consequences for skill in statistical seasonal forecasts, such as has
600 been the case with the ENSO-Indian Monsoon relationship (Kumar *et al* 1999).
601 Teleconnections between ENSO and Australian climate have some decadal-scale variability
602 related to the Interdecadal Pacific Oscillation (Power *et al* 2006, King *et al* 2013a, Cai and
603 van Rensch 2012, Lim *et al* 2017) so there is the possibility that the 23-year hindcast period
604 does not optimally represent the recent Australian climate and its variability. For the next
605 version of ACCESS-S (version 2), there will be a longer hindcast period of at least 30 years.
606 While it is promising that the teleconnections between climate modes and mean and extreme

rainfall indices are broadly captured in the 23-year ACCESS-S1 hindcast, further analysis of teleconnections using a longer hindcast would be useful.

Overall, in this analysis we have found that sub-seasonal prediction of some rainfall indices in Australia may be viable using the BoM operational model, ACCESS-S1, but that performance decreases rapidly beyond the first forecast month. A substantial component of forecast performance at lead-0 is due to skill on the timeframe of weather prediction, so seasonal prediction is unlikely to be possible but sub-seasonal outlooks, extending beyond the current forecasts of likelihood of above or below-average total rainfall, may be useful. Forecasts based on indices such as the probability of above- or below-average number of wet days and intensity of the wettest day are possible. Further work will be needed to determine the usefulness of such indices in sub-seasonal outlooks.

Acknowledgements

We thank the editor for handling our manuscript and we thank Nicholas Klingaman and an anonymous reviewer for their constructive feedback on our paper. Andrew King and Todd Lane were funded by the Australian Research Council (DE180100638 and CE170100023 respectively). Debra Hudson, Eun-Pa Lim, Andrew Marshall and Harry Hendon's contribution is part of the Forewarned is Forearmed project, which is supported by funding from the the Australian Government Department of Agriculture as part of its Rural Research and Development for Profit programme. The work was undertaken with the assistance of resources from the National Computational Infrastructure (NCI), which is supported by the Australian Government.

References

Alves O, Wang G, Zhong A, Smith N, Tseitkin F, Warren G, Schiller A, Godfrey S and Meyers G 2003 POAMA: Bureau of Meteorology operational coupled model seasonal

631 forecast system *National Drought Forum* (Brisbane) pp 49–56

632 Australian Business Roundtable for Disaster Resilience & Safer Communities 2016 *The*
633 *economic cost of the social impact of natural disasters* (Sydney) Online:
634 http://australianbusinessroundtable.com.au/assets/documents/Report - Social
635 costs/Report - The economic cost of the social impact of natural disasters.pdf

636 Bhend J, Mahlstein I and Liniger M A 2017 Predictive skill of climate indices compared to
637 mean quantities in seasonal forecasts *Q. J. R. Meteorol. Soc.* **143** 184–94 Online:
638 http://doi.wiley.com/10.1002/qj.2908

639 Bureau of Meteorology 2019 *Operational Implementation of ACCESS-S1 Forecast Post-*
640 *Processing* (Melbourne) Online:
641 http://www.bom.gov.au/australia/charts/bulletins/opsull-124-ext.pdf

642 de Burgh-Day C O, Spillman C M, Stevens C, Alves O and Rickard G 2019 Predicting
643 seasonal ocean variability around New Zealand using a coupled ocean-atmosphere
644 model *New Zeal. J. Mar. Freshw. Res.* **53** 201–21 Online:
645 https://www.tandfonline.com/doi/full/10.1080/00288330.2018.1538052

646 Cai W and van Rensch P 2012 The 2011 southeast Queensland extreme summer rainfall: A
647 confirmation of a negative Pacific Decadal Oscillation phase? *Geophys. Res. Lett.* **39**
648 n/a-n/a Online: http://doi.wiley.com/10.1029/2011GL050820

649 Camp J, Wheeler M C, Hendon H H, Gregory P A, Marshall A G, Tory K J, Watkins A B,
650 MacLachlan C and Kuleshov Y 2018 Skilful multiweek tropical cyclone prediction in
651 ACCESS-S1 and the role of the MJO *Q. J. R. Meteorol. Soc.* **144** 1337–51 Online:
652 http://doi.wiley.com/10.1002/qj.3260

653 Catto J L, Nicholls N and Jakob C 2012 North Australian Sea Surface Temperatures and the

El Niño–Southern Oscillation in Observations and Models *J. Clim.* **25** 5011–29 Online: http://journals.ametsoc.org/doi/abs/10.1175/JCLI-D-11-00311.1

Cavicchia L, Pepler A, Dowdy A and Walsh K 2019 A Physically Based Climatology of the Occurrence and Intensification of Australian East Coast Lows *J. Clim.* **32** 2823–41 Online: http://journals.ametsoc.org/doi/10.1175/JCLI-D-18-0549.1

Cottrill A, Hendon H H, Lim E-P, Langford S, Shelton K, Charles A, McClymont D, Jones D and Kuleshov Y 2013 Seasonal Forecasting in the Pacific Using the Coupled Model POAMA-2 *Weather Forecast.* **28** 668–80 Online: http://journals.ametsoc.org/doi/abs/10.1175/WAF-D-12-00072.1

Donat M G, Alexander L V., Yang H, Durre I, Vose R, Dunn R J H, Willett K M, Aguilar E, Brunet M, Caesar J, Hewitson B, Jack C, Klein Tank A M G, Kruger A C, Marengo J, Peterson T C, Renom M, Oria Rojas C, Rusticucci M, Salinger J, Elrayah A S, Sekele S S, Srivastava A K, Trewin B, Villarroel C, Vincent L A, Zhai P, Zhang X and Kitching S 2013 Updated analyses of temperature and precipitation extreme indices since the beginning of the twentieth century: The HadEX2 dataset *J. Geophys. Res. Atmos.* **118** 2098–118 Online: http://doi.wiley.com/10.1002/jgrd.50150

Dowdy A J, Qi L, Jones D, Ramsay H, Fawcett R and Kuleshov Y 2012 Tropical Cyclone Climatology of the South Pacific Ocean and Its Relationship to El Niño–Southern Oscillation *J. Clim.* **25** 6108–22 Online: http://journals.ametsoc.org/doi/abs/10.1175/JCLI-D-11-00647.1

Drosdowsky W and Chambers L E 2000 Near-Global Sea Surface Temperature Anomalies as Predictors of Australian Seasonal Rainfall *J. Clim.* **14** 1677–87 Online: https://journals.ametsoc.org/doi/pdf/10.1175/1520-0442%282001%29014%3C1677%3ANACNGS%3E2.0.CO%3B2

678 Ebert E . and McBride J . 2000 Verification of precipitation in weather systems:
679 determination of systematic errors *J. Hydrol.* **239** 179–202 Online:
680 https://www.sciencedirect.com/science/article/pii/S0022169400003437

681 Evans J P and Boyer-Souchet I 2012 Local sea surface temperatures add to extreme
682 precipitation in northeast Australia during La Niña *Geophys. Res. Lett.* **39** n/a-n/a
683 Online: http://doi.wiley.com/10.1029/2012GL052014

684 Hartmann H C, Pagano T C, Sorooshian S and Bales R 2002 Confidence Builders: Evaluating
685 Seasonal Climate Forecasts from User Perspectives *Bull. Am. Meteorol. Soc.* **83** 683–98
686 Online: http://journals.ametsoc.org/doi/abs/10.1175/1520-
687 0477%282002%29083%3C0683%3ACBESCF%3E2.3.CO%3B2

688 Haylock M and Nicholls N 2000 Trends in extreme rainfall indices for an updated high
689 quality data set for Australia, 1910-1998 *Int. J. Climatol.* **20** 1533–41 Online:
690 http://doi.wiley.com/10.1002/1097-
691 0088%2820001115%2920%3A13%3C1533%3A%3AAID-JOC586%3E3.0.CO%3B2-J

692 Hendon H H, Lim E-P and Nguyen H 2014 Seasonal Variations of Subtropical Precipitation
693 Associated with the Southern Annular Mode *J. Clim.* **27** 3446–60 Online:
694 http://journals.ametsoc.org/doi/abs/10.1175/JCLI-D-13-00550.1

695 van den Honert R C and McAneney J 2011 The 2011 Brisbane Floods: Causes, Impacts and
696 Implications *Water* **3** 1149–73 Online: http://www.mdpi.com/2073-4441/3/4/1149

697 Hudson D, Alves O, Hendon H H, Lim E-P, Liu G, Luo J-J, Maclachlan C, Marshall A G,
698 Shi L, Wang G, Wedd R, Young G, Zhao M and Zhou X 2017 ACCESS-S1: The new
699 Bureau of Meteorology multi-week to seasonal prediction system *J. South. Hemisph.*
700 *Earth Syst. Sci.* **673** 132–59 Online:
701 http://www.bom.gov.au/jshess/docs/2017/Hudson.pdf

Hudson D, Alves O, Hendon H H and Marshall A G 2011 Bridging the gap between weather and seasonal forecasting: intraseasonal forecasting for Australia *Q. J. R. Meteorol. Soc.* **137** 673–89 Online: http://doi.wiley.com/10.1002/qj.769

Hudson D and Marshall A G 2016 *Extending the Bureau's heatwave forecast to multi-week timescales* (Melbourne) Online: http://www.bom.gov.au/research/publications/researchreports/BRR-016.pdf

Jones D A, Wang W and Fawcett R 2009 High-quality spatial climate data-sets for Australia *Aust. Meteorol. Oceanogr. J.* **58** 233–48 Online: http://www.bom.gov.au/jshess/docs/2009/jones_hres.pdf

King A D, Alexander L V and Donat M G 2013a Asymmetry in the response of eastern Australia extreme rainfall to low-frequency Pacific variability *Geophys. Res. Lett.* **40**

King A D, Alexander L V and Donat M G 2013b The efficacy of using gridded data to examine extreme rainfall characteristics: A case study for Australia *Int. J. Climatol.* **33**

King A D, Klingaman N P, Alexander L V., Donat M G, Jourdain N C and Maher P 2014 Extreme Rainfall Variability in Australia: Patterns, Drivers, and Predictability* *J. Clim.* **27** 6035–50 Online: http://journals.ametsoc.org/doi/abs/10.1175/JCLI-D-13-00715.1

Klingaman N P, Woolnough S J and Syktus J 2013 On the drivers of inter-annual and decadal rainfall variability in Queensland, Australia *Int. J. Climatol.* **33** 2413–30 Online: http://doi.wiley.com/10.1002/joc.3593

Kuleshov Y, Qi L, Fawcett R and Jones D 2008 On tropical cyclone activity in the Southern Hemisphere: Trends and the ENSO connection *Geophys. Res. Lett.* **35** L14S08 Online: http://doi.wiley.com/10.1029/2007GL032983

Kumar K K, Rajagopalan B and Cane M A 1999 On the weakening relationship between the

725 indian monsoon and ENSO *Science* **284** 2156–9 Online:
726 http://www.ncbi.nlm.nih.gov/pubmed/10381876

727 Lee S-S, Moon J-Y, Wang B and Kim H-J 2017 Subseasonal Prediction of Extreme
728 Precipitation over Asia: Boreal Summer Intraseasonal Oscillation Perspective *J. Clim.*
729 **30** 2849–65 Online: http://journals.ametsoc.org/doi/10.1175/JCLI-D-16-0206.1

730 Lim E-P and Hendon H H 2015 Understanding and predicting the strong Southern Annular
731 Mode and its impact on the record wet east Australian spring 2010 *Clim. Dyn.* **44** 2807–
732 24 Online: http://link.springer.com/10.1007/s00382-014-2400-5

733 Lim E-P, Hendon H H, Zhao M and Yin Y 2017 Inter-decadal variations in the linkages
734 between ENSO, the IOD and south-eastern Australian springtime rainfall in the past
735 30 years *Clim. Dyn.* **49** 97–112 Online: http://link.springer.com/10.1007/s00382-016-
736 3328-8

737 MacLachlan C, Arribas A, Peterson K A, Maidens A, Fereday D, Scaife A A, Gordon M,
738 Vellinga M, Williams A, Comer R E, Camp J, Xavier P and Madec G 2015 Global
739 Seasonal forecast system version 5 (GloSea5): a high-resolution seasonal forecast
740 system *Q. J. R. Meteorol. Soc.* **141** 1072–84 Online:
741 http://doi.wiley.com/10.1002/qj.2396

742 Marshall A G and Hendon H H 2019 Multi-week prediction of the Madden–Julian oscillation
743 with ACCESS-S1 *Clim. Dyn.* **52** 2513–28 Online:
744 http://link.springer.com/10.1007/s00382-018-4272-6

745 Marshall A G, Hudson D, Wheeler M C, Alves O, Hendon H H, Pook M J and Risbey J S
746 2014 Intra-seasonal drivers of extreme heat over Australia in observations and POAMA-
747 2 *Clim. Dyn.* **43** 1915–37 Online: http://link.springer.com/10.1007/s00382-013-2016-1

McBride J L and Nicholls N 1983 Seasonal Relationships between Australian Rainfall and the Southern Oscillation *Mon. Weather Rev.* **111** 1998–2004 Online: http://journals.ametsoc.org/doi/abs/10.1175/1520-0493%281983%29111%3C1998%3ASRBARA%3E2.0.CO%3B2

Mills G A, Webb R, Davidson N E, Kepert J, Seed A and Abbs D 2010 *The Pasha Bulker east coast low of 8 June 2007* Online: https://www.researchgate.net/profile/Jeffrey_Kepert/publication/277295660_Subjects_Meteorology--Research_Climatic_changes--Research/links/55c0204708ae092e9666a6db.pdf

Min S-K, Cai W and Whetton P 2013 Influence of climate variability on seasonal extremes over Australia *J. Geophys. Res. Atmos.* **118** 643–54 Online: http://doi.wiley.com/10.1002/jgrd.50164

Nicholls N 1979 A Possible Method for Predicting Seasonal Tropical Cyclone Activity in the Australian Region *Mon. Weather Rev.* **107** 1221–4 Online: http://journals.ametsoc.org/doi/abs/10.1175/1520-0493%281979%29107%3C1221%3AAPMFPS%3E2.0.CO%3B2

Nicholls N 1985 Predictability of Interannual Variations of Australian Seasonal Tropical Cyclone Activity *Mon. Weather Rev.* **113** 1144–9 Online: http://journals.ametsoc.org/doi/abs/10.1175/1520-0493%281985%29113%3C1144%3APOIVOA%3E2.0.CO%3B2

Nicholls N 1983 The potential for long-range prediction of seasonal mean temperature in Australia *Aust. Meteorol. Mag.* **31** 203–7

Nicholls N 1984 The Southern Oscillation, sea-surface-temperature, and interannual fluctuations in Australian tropical cyclone activity *J. Climatol.* **4** 661–70 Online:

http://doi.wiley.com/10.1002/joc.3370040609

Nicholls N, Drosdowsky W and Lavery B 1997 Australian rainfall variability and change *Weather* **52** 66–72 Online: http://doi.wiley.com/10.1002/j.1477-8696.1997.tb06274.x

Nicholls N and Woodcock F 1981 Verification of an empirical long-range weather forecasting technique *Q. J. R. Meteorol. Soc.* **107** 973–6 Online: http://doi.wiley.com/10.1002/qj.49710745415

Pepler A S, Díaz L B, Prodhomme C and Doblas-Reyes F J 2015a The ability of a multi-model seasonal forecasting ensemble to forecast the frequency of warm, cold and wet extremes *Weather Clim. Extrem.* **9** 68–77 Online: https://www.sciencedirect.com/science/article/pii/S2212094715300062

Pepler A S, Di Luca A, Ji F, Alexander L V., Evans J P and Sherwood S C 2015b Impact of Identification Method on the Inferred Characteristics and Variability of Australian East Coast Lows *Mon. Weather Rev.* **143** 864–77 Online: http://journals.ametsoc.org/doi/10.1175/MWR-D-14-00188.1

Power S, Haylock M, Colman R and Wang X 2006 The Predictability of Interdecadal Changes in ENSO Activity and ENSO Teleconnections *J. Clim.* **19** 4755–71 Online: http://journals.ametsoc.org/doi/abs/10.1175/JCLI3868.1

Quayle E T 1929 Long range rainfall forecasting from tropical (Darwin) air pressures *Proc. R. Soc. Victoria* **41** 160–4

Rayner N A, Parker D E, Horton E B, Folland C K, Alexander L V., Rowell D P, Kent E C and Kaplan A 2003 Global analyses of sea surface temperature, sea ice, and night marine air temperature since the late nineteenth century *J. Geophys. Res.* **108** 4407 Online: http://doi.wiley.com/10.1029/2002JD002670

795 Risbey J S, Pook M J, McIntosh P C, Wheeler M C and Hendon H H 2009 On the Remote
796 Drivers of Rainfall Variability in Australia *Mon. Weather Rev.* **137** 3233–53 Online:
797 http://journals.ametsoc.org/doi/abs/10.1175/2009MWR2861.1

798 Roberts N 2008 Assessing the spatial and temporal variation in the skill of precipitation
799 forecasts from an NWP model *Meteorol. Appl.* **15** 163–9 Online:
800 http://doi.wiley.com/10.1002/met.57

801 Saji N H, Goswami B N, Vinayachandran P N and Yamagata T 1999 A dipole mode in the
802 tropical Indian Ocean *Nature* **401** 360–3 Online: http://www.nature.com/articles/43854

803 Sillmann J, Kharin V V., Zhang X, Zwiers F W and Bronaugh D 2013 Climate extremes
804 indices in the CMIP5 multimodel ensemble: Part 1. Model evaluation in the present
805 climate *J. Geophys. Res. Atmos.* **118** 1716–33 Online:
806 http://doi.wiley.com/10.1002/jgrd.50203

807 Sillmann J, Thorarinsdottir T, Keenlyside N, Schaller N, Alexander L V., Hegerl G,
808 Seneviratne S I, Vautard R, Zhang X and Zwiers F W 2017 Understanding, modeling
809 and predicting weather and climate extremes: Challenges and opportunities *Weather*
810 *Clim. Extrem.* **18** 65–74 Online:
811 https://www.sciencedirect.com/science/article/pii/S2212094717300440#bib102

812 Smith G and Spillman C 2019 New high-resolution sea surface temperature forecasts for
813 coral reef management on the Great Barrier Reef *Coral Reefs* 1–18 Online:
814 http://link.springer.com/10.1007/s00338-019-01829-1

815 Stone R C, Hammer G L and Marcussen T 1996 Prediction of global rainfall probabilities
816 using phases of the Southern Oscillation Index *Nature* **384** 252–5 Online:
817 http://www.nature.com/doifinder/10.1038/384252a0

The Centre for International Economics 2014a *Analysis of the benefits of improved seasonal climate forecasting* Online: http://www.managingclimate.gov.au/wp-content/uploads/2014/05/MCV-CIE-report-Value-of-improved-forecasts-non-agriculture-2014.pdf

The Centre for International Economics 2014b *Analysis of the benefits of improved seasonal climate forecasting for agriculture* Online: http://www.managingclimate.gov.au/wp-content/uploads/2014/06/MCV-CIE-report-Value-of-improved-forecasts-agriculture-2014.pdf

Vitart F, Cunningham C, DeFlorio M, Dutra E, Ferranti L, Golding B, Hudson D, Jones C, Lavaysse C, Robbins J and Tippett M K 2019 Sub-seasonal to Seasonal Prediction of Weather Extremes *Sub-Seasonal to Seas. Predict.* 365–86 Online: https://www.sciencedirect.com/science/article/pii/B9780128117149000176

Wilks D S 2010 Sampling distributions of the Brier score and Brier skill score under serial dependence *Q. J. R. Meteorol. Soc.* **136** 2109–18 Online: http://doi.wiley.com/10.1002/qj.709

Wilks D S 2011 *Statistical methods in the atmospheric sciences* (Elsevier/Academic Press)

Zhang X, Alexander L, Hegerl G C, Jones P, Tank A K, Peterson T C, Trewin B and Zwiers F W 2011 Indices for monitoring changes in extremes based on daily temperature and precipitation data *Wiley Interdiscip. Rev. Clim. Chang.* **2** 851–70 Online: http://doi.wiley.com/10.1002/wcc.147

Ziervogel G and Downing T E 2004 Stakeholder Networks: Improving Seasonal Climate Forecasts *Clim. Change* **65** 73–101 Online: http://link.springer.com/10.1023/B:CLIM.0000037492.18679.9e

841

Figures and Tables

Table 1. Mean and extreme rainfall indices considered in this analysis. These indices were examined in the observational-based analysis and the indices listed in italics were investigated further using ACCESS-S.

Index Name	Description	Units	Type of Index
PRCPTOT	*Total Rainfall*	*mm*	*Mean*
Rx1day	*Maximum 1-day rainfall*	*mm*	*Intensity*
R90PTOT	*Rainfall on days above climatological 90th percentile*	*mm*	*Intensity*
WD	*Number of wet days (>1mm)*	*Number of days*	*Frequency*
R90P	*Number of days above climatological 90th percentile*	*Number of days*	*Frequency*
R10mm	*Number of days above 10mm*	*Number of days*	*Frequency*
Rx1C	Contribution of wettest day to total rainfall	%	Contribution

Table 2. Months used in composites of forecasts during ENSO, IOD and North Australian SST mode phases.

Climate Mode	Calendar months analysed	Years extracted in positive phase	Years extracted in negative phase
ENSO (Niño-3.4)	October	1991, 1994, 1997, 2002, 2009	1998, 1999, 2007, 2010, 2011
IOD (DMI)	September	1994, 1997, 2002, 2006, 2012	1992, 1996, 1998, 2005, 2010
N. Australian SSTs	July	1990, 1996, 1998, 2009, 2010	1991, 1993, 1994, 1997, 2000
SAM (Marshall index)	November	1992, 1998, 1999, 2001, 2010	1994, 1996, 1997, 2000, 2011

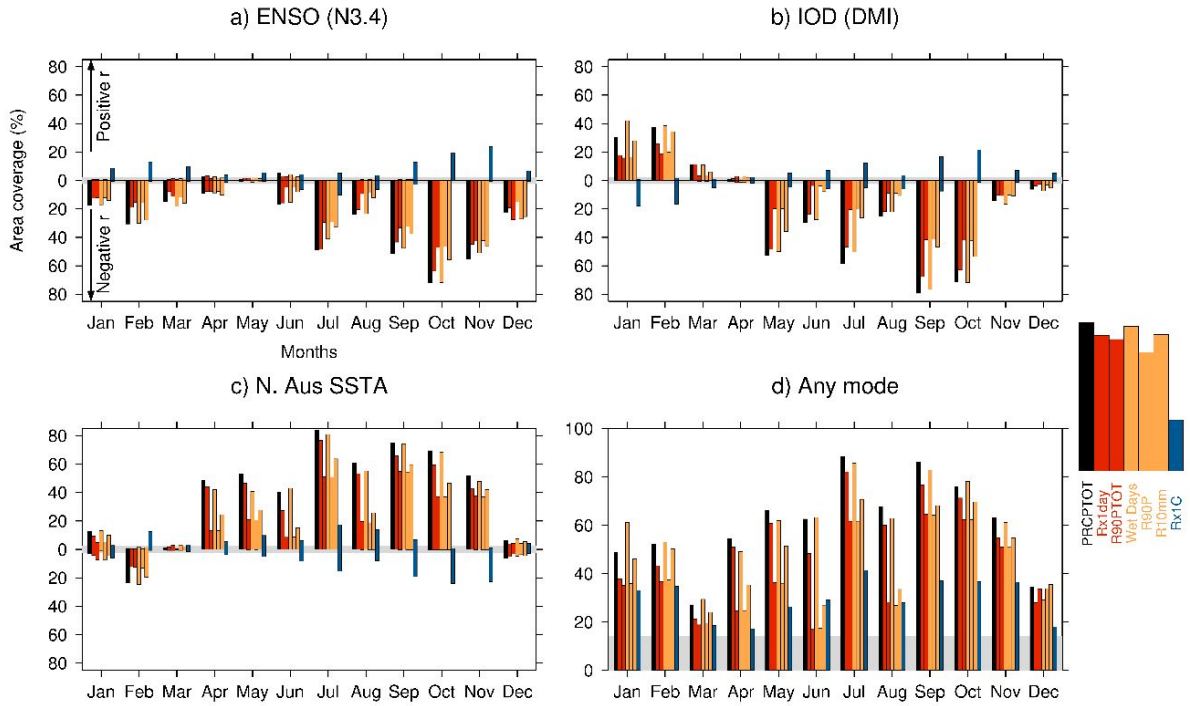

850

851 **Figure 1.** Bar graphs showing the area of Australia with significant concurrent Spearman-
852 rank correlations (p-value < 0.05) between mean and extreme rainfall indices and a) Niño-
853 3.4, b) DMI, c) N. Australian SSTs, and d) any of the three climate modes. Bars in a-c are
854 plotted either above or below the zero line for positive or negative correlations respectively.
855 The grey region indicates the area of significant correlations that might be expected by
856 chance. The legend on the right indicates which bars correspond to which indices with mean
857 rainfall in black, intensity-based indices in red, frequency-based indices in orange and a
858 contribution-based index in blue.

859

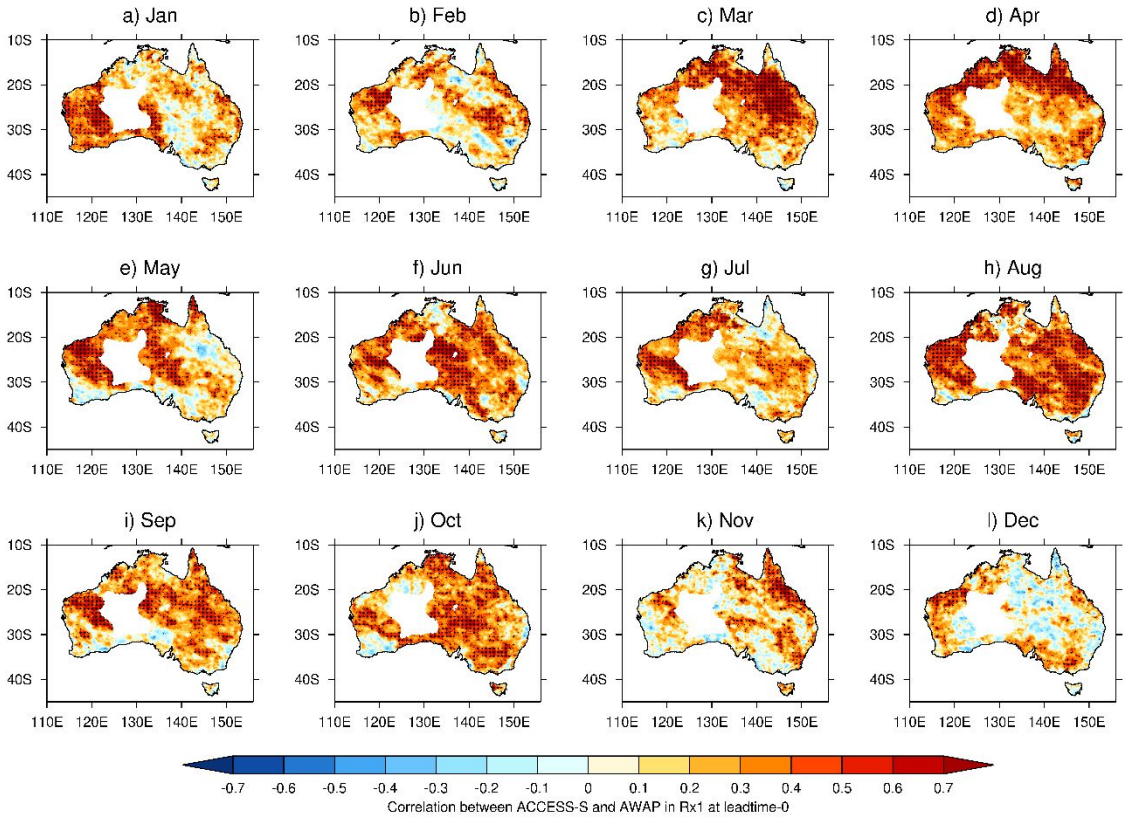

860

861 **Figure 2.** Spearman's rank correlation coefficients in Rx1day between AWAP and the

862 ensemble median ACCESS-S1 value at leadtime-0 for each calendar month from 1990-2012.

863 Stippling indicates correlations significant at the 5% level.

864

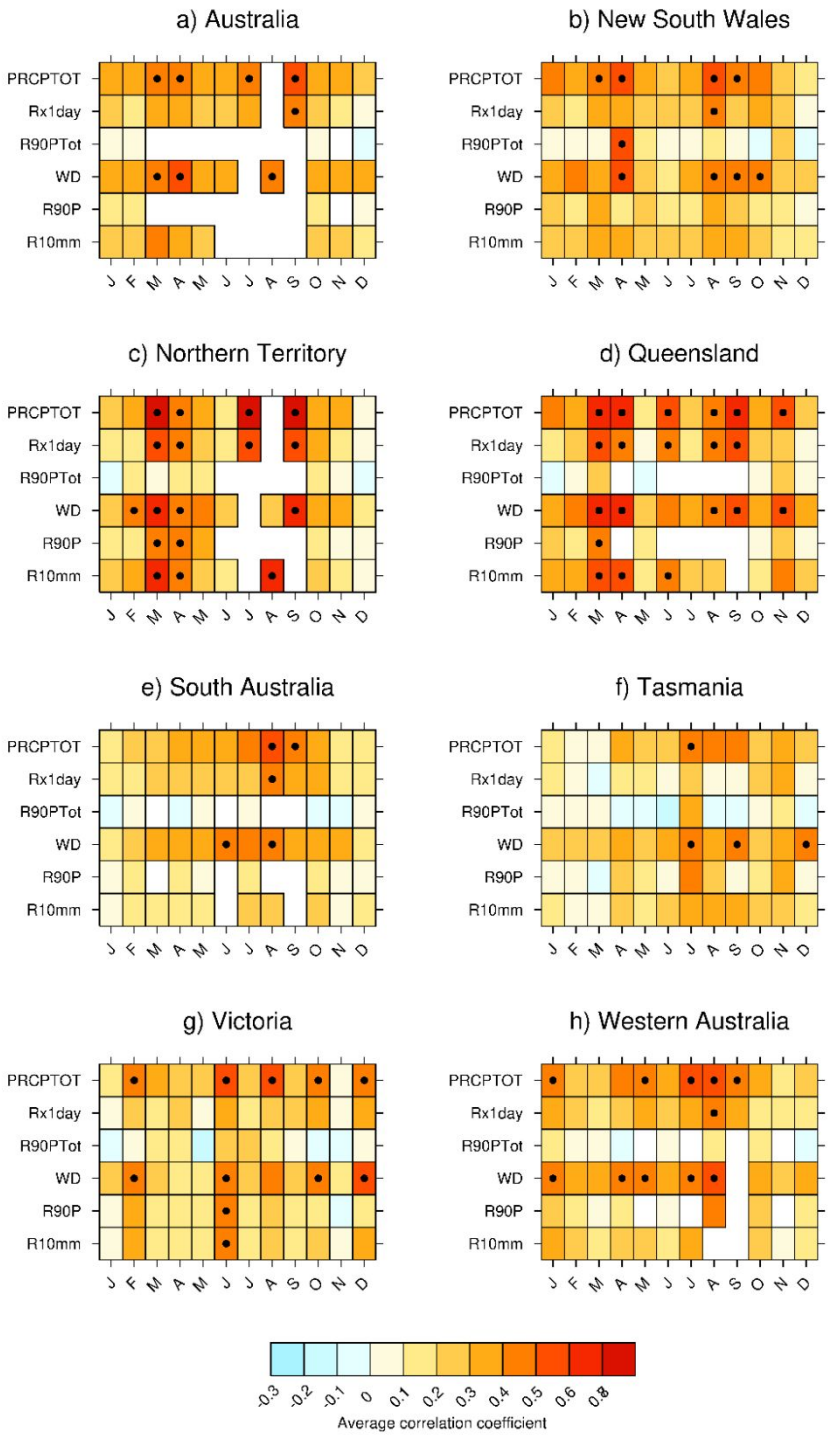

865

866 **Figure 3.** Area-average correlation coefficient matrices for each state of Australia in each
867 calendar month and index at leadtime-0. Black dots indicate correlations significant at the 5%
868 level. These Pearson correlation coefficients are derived by applying the Fisher Z-transform
869 and area-averaging on Z-scores. Grid cells in white show areas where the index has too few
870 non-zero values for reliable correlation calculation.

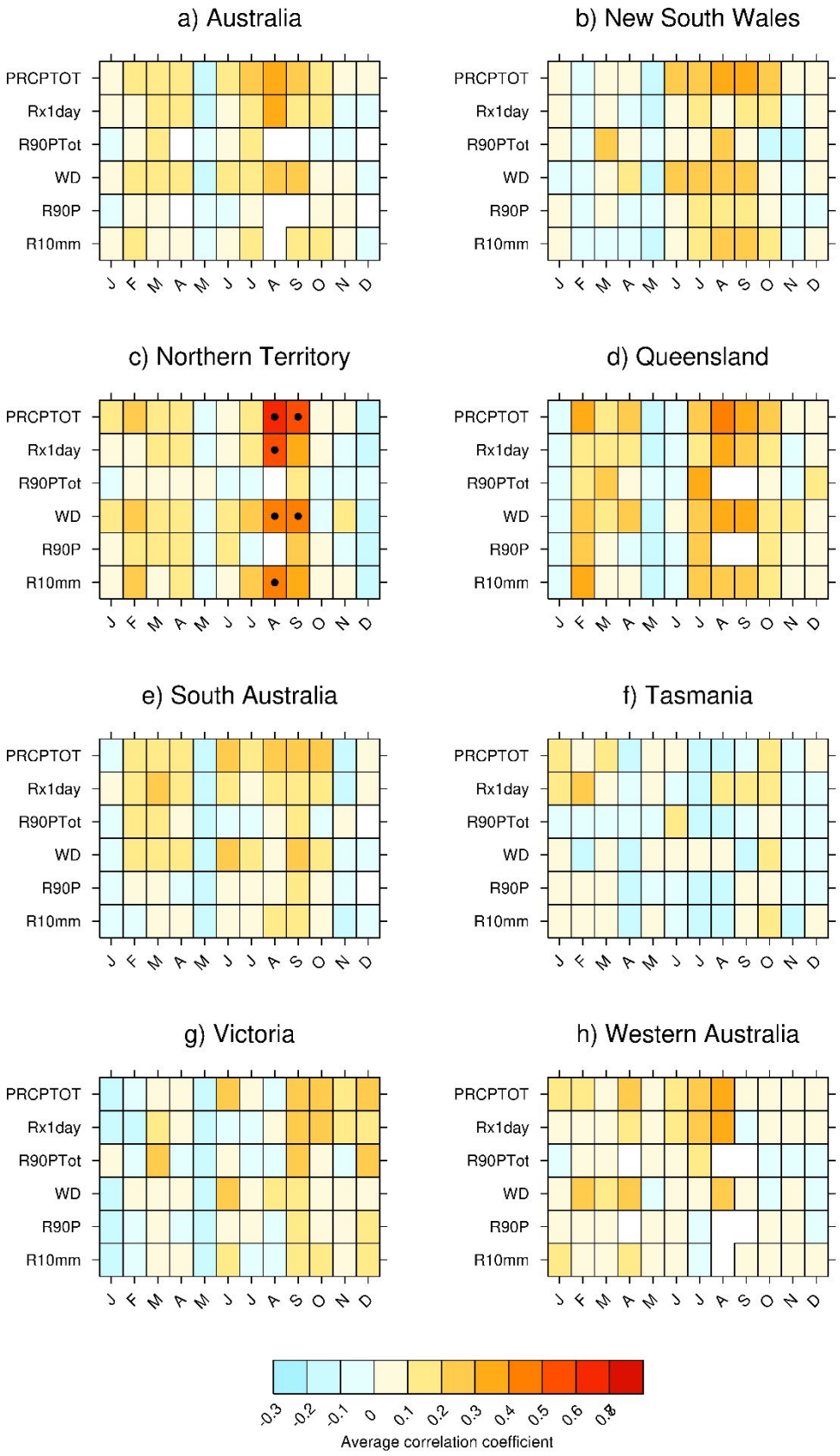

871

872 **Figure 4.** As Figure 3 but for lead-1 month correlation coefficients.

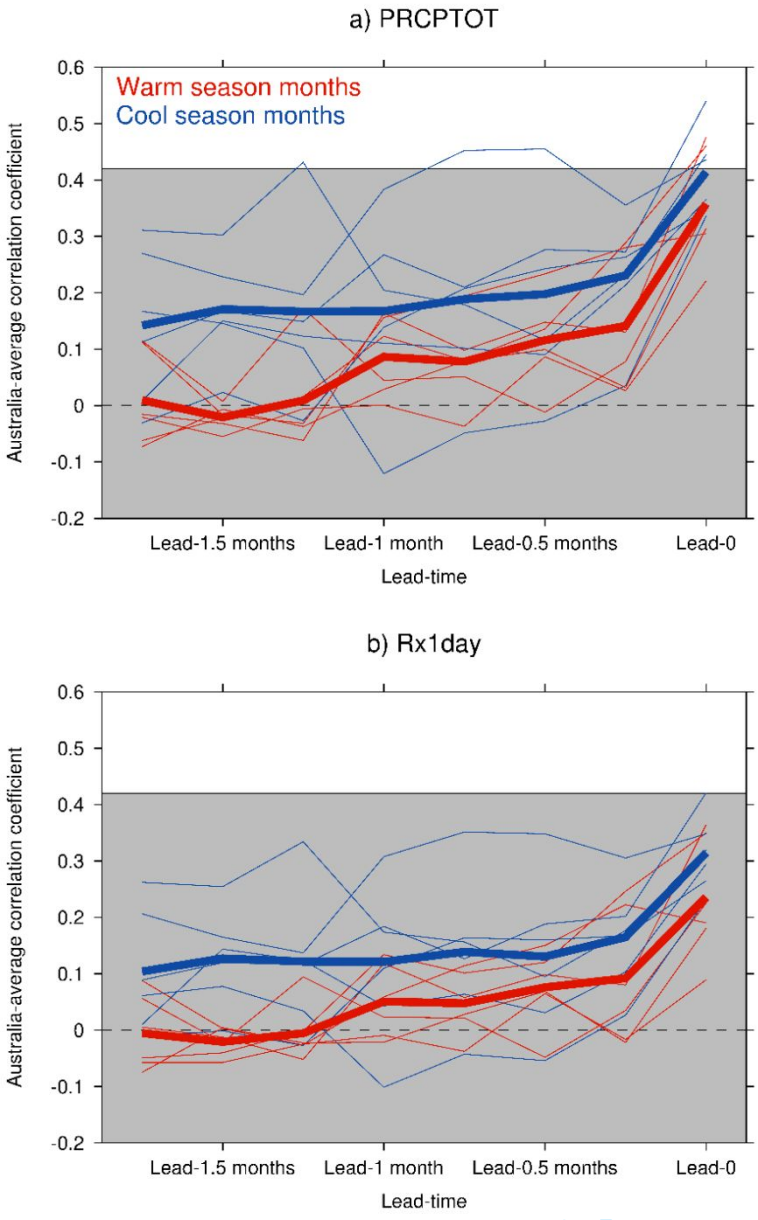

873

874 **Figure 5.** Australian-average correlation coefficients between ACCESS-S and AWAP
875 calculated for each calendar month at every lead-time from 1.75 months in advance to lead-0
876 for a) PRCPTOT and b) Rx1day. Each thin line represents a different calendar month with
877 months during the warm season marked in red and cool season months in blue. These Pearson
878 correlation coefficients are derived by applying the Fisher Z-transform and area-averaging on
879 Z-scores. The thicker lines represent warm and cool season average correlations at each lead-
880 time computed by averaging the Z-scores from each month at that lead-time. The grey area
881 shows correlations non-significant at the 5% level.

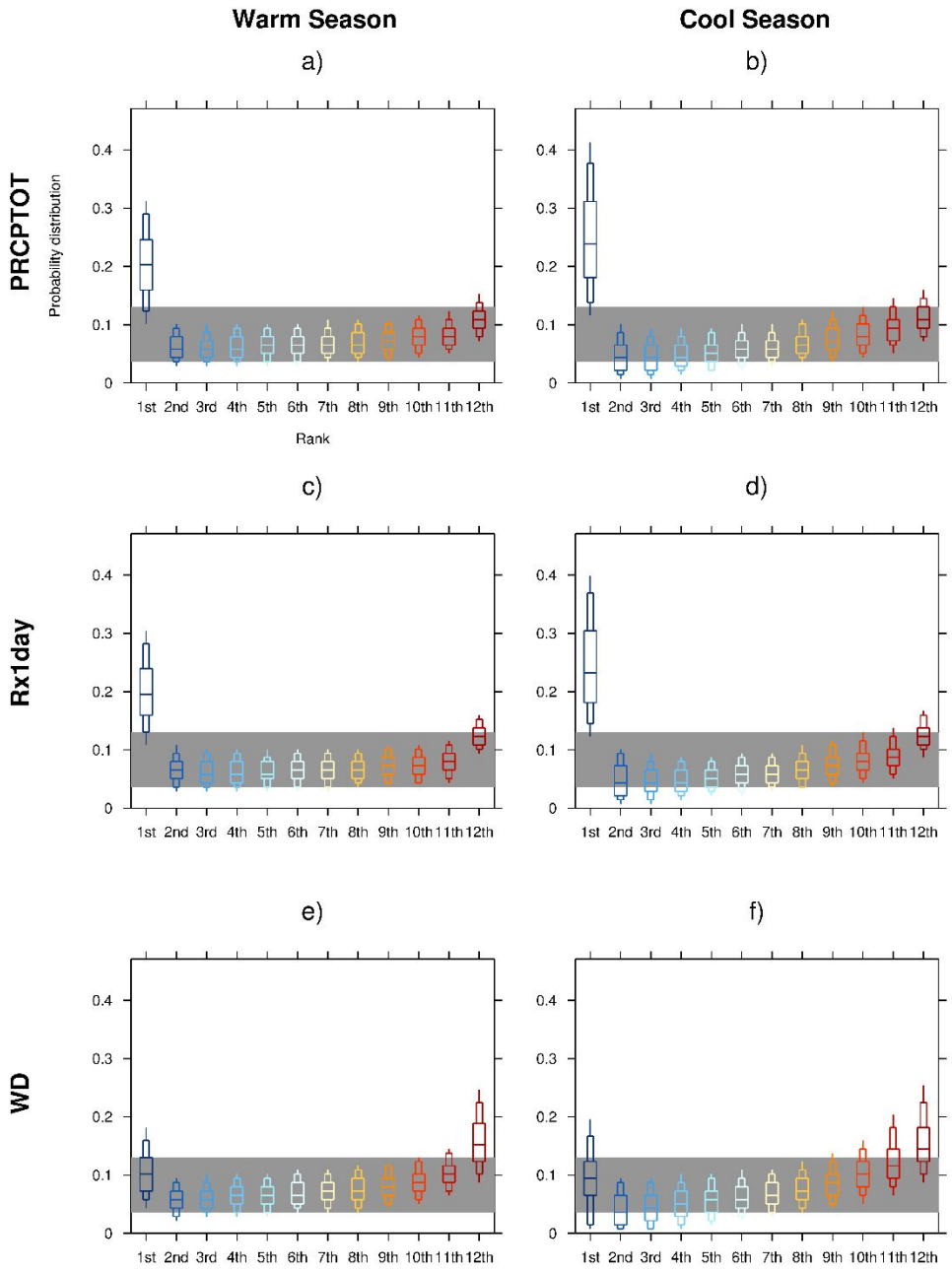

882

883 **Figure 6.** Rank Histograms showing the frequency of ranks of the observed value relative to
884 the ACCESS-S1 ensemble in locations across Australia. The box-plots show the frequency at
885 the median location with the large box representing the interquartile range, the narrower box
886 representing the 10^{th}-90^{th} percentile range, and the whiskers showing the 5^{th}-95^{th} percentile
887 locations. The grey zone represents an estimate of the 95% confidence interval of rank
888 frequencies that could be expected by random chance for the same sample size as is available
889 here.

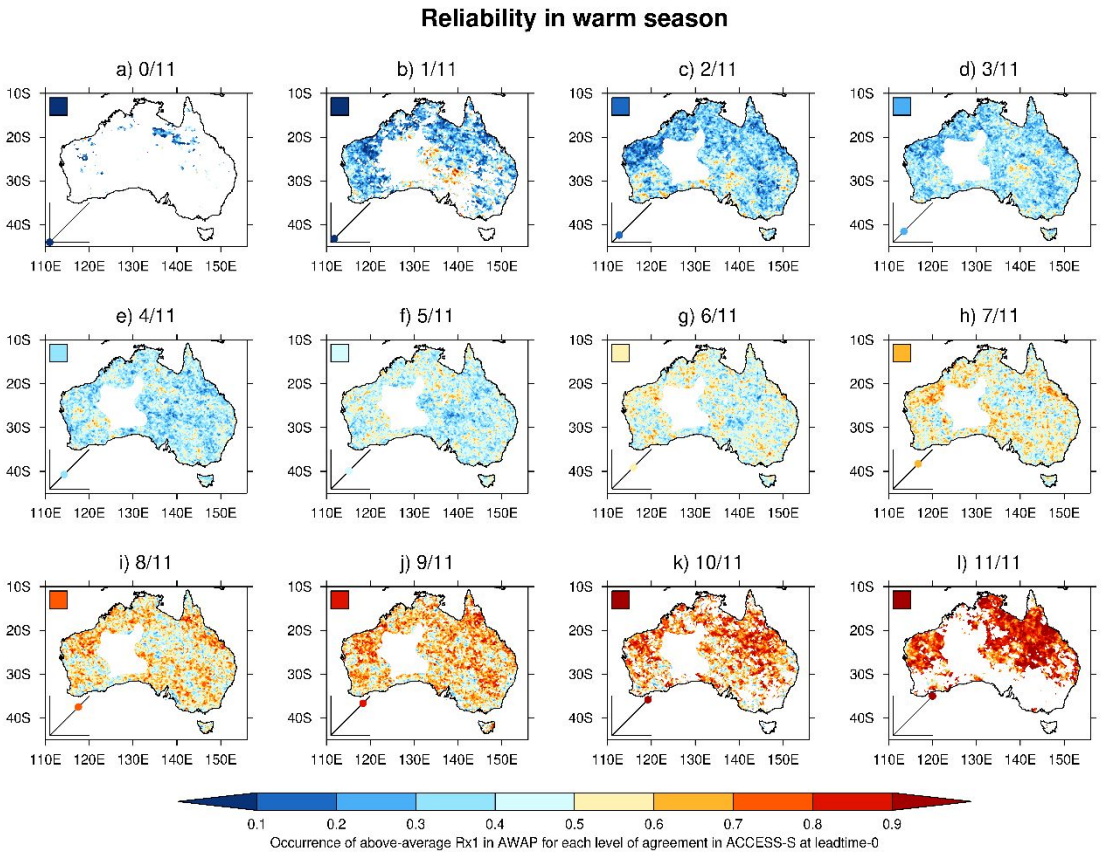

890

891 **Figure 7.** Maps representing the reliability in Rx1day lead-0 predictions in the warm season
892 (Nov-Apr). For cases when each possible fraction of the ACCESS-S1 ensemble is above
893 average, the fraction of corresponding observed values that are above average is shown. The
894 fraction is only shown where there are at least five occurrences where ACCESS-S1 has the
895 fraction of above-average ensemble members considered. The expected colour if ACCESS-
896 S1 is performing well is shown in the top left of each plot and a graphical representation of
897 the point on a reliability diagram being investigated is shown in the bottom-left of each plot.

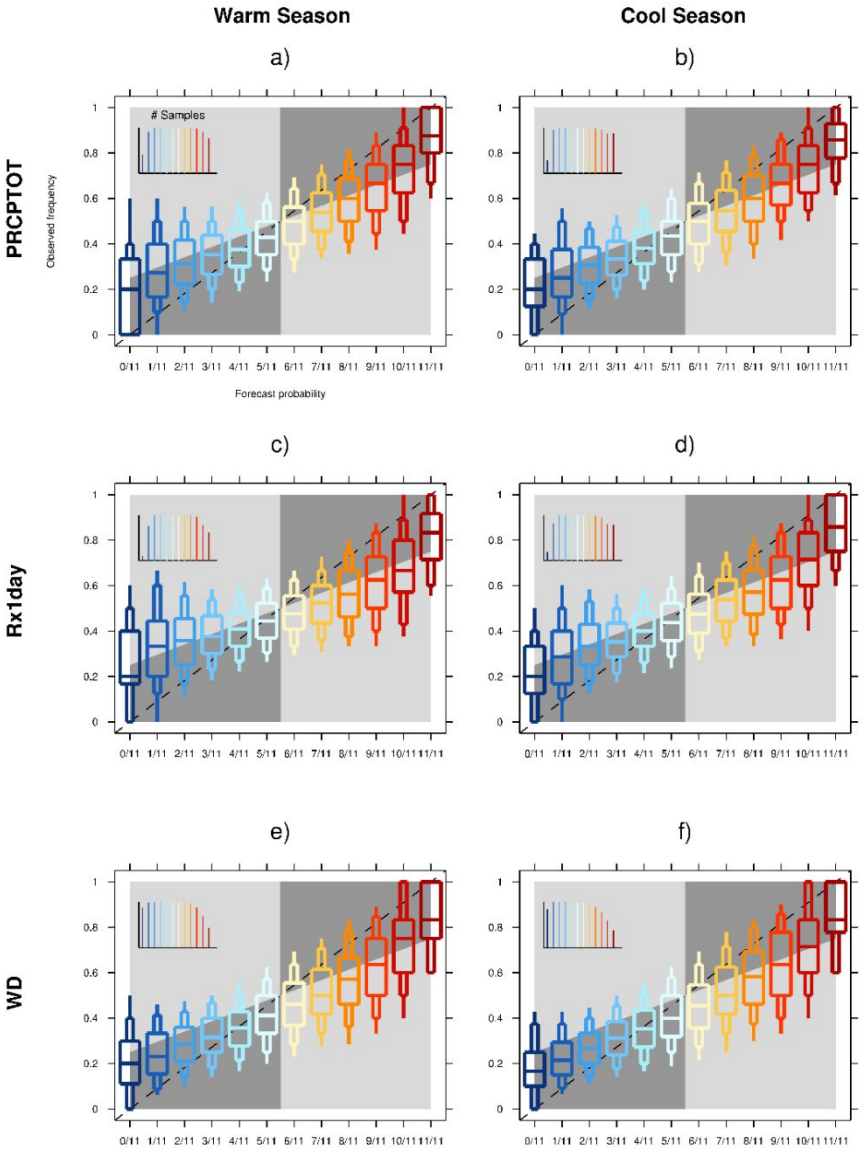

898

899 **Figure 8.** Reliability diagrams aggregating locations across Australia. For each forecast
900 probability of above-average conditions in a), b) PRCPTOT, c), d) Rx1day, and e), f) WD in
901 the warm and cool season respectively, the corresponding observed occurrence is shown with
902 the box-plot representing the range of occurrences across Australia. The box plots use the
903 same percentiles as those in Figure 6. The colours are chosen to match those in Figure 7.
904 Miniature graphs in the top-left of each plot indicate the number of locations contributing to
905 each box-plot as a proportion of the maximum number. The dark grey area shows where a
906 positive contribution to Brier Skill Score is made. The 1:1 line is shown as a dashed black
907 line.

908

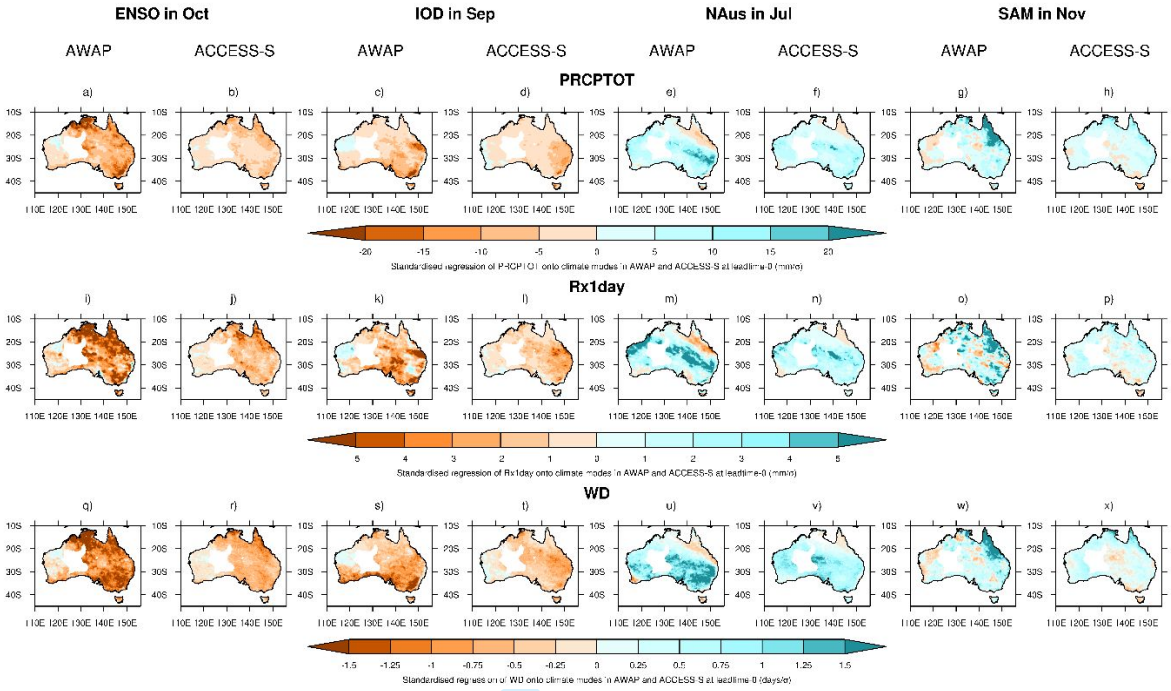

909

910 **Figure 9.** Standardised regression coefficients of mean and extreme rainfall indices onto each
911 climate mode index in the 1990-2012 period for selected months with strong mean and
912 extreme rainfall relationships to these modes in AWAP and the ACCESS-S1 ensemble
913 median respectively. Regression coefficients are shown for a)-h) PRCPTOT, i)-p) Rx1day,
914 and q)-x) WD.

915

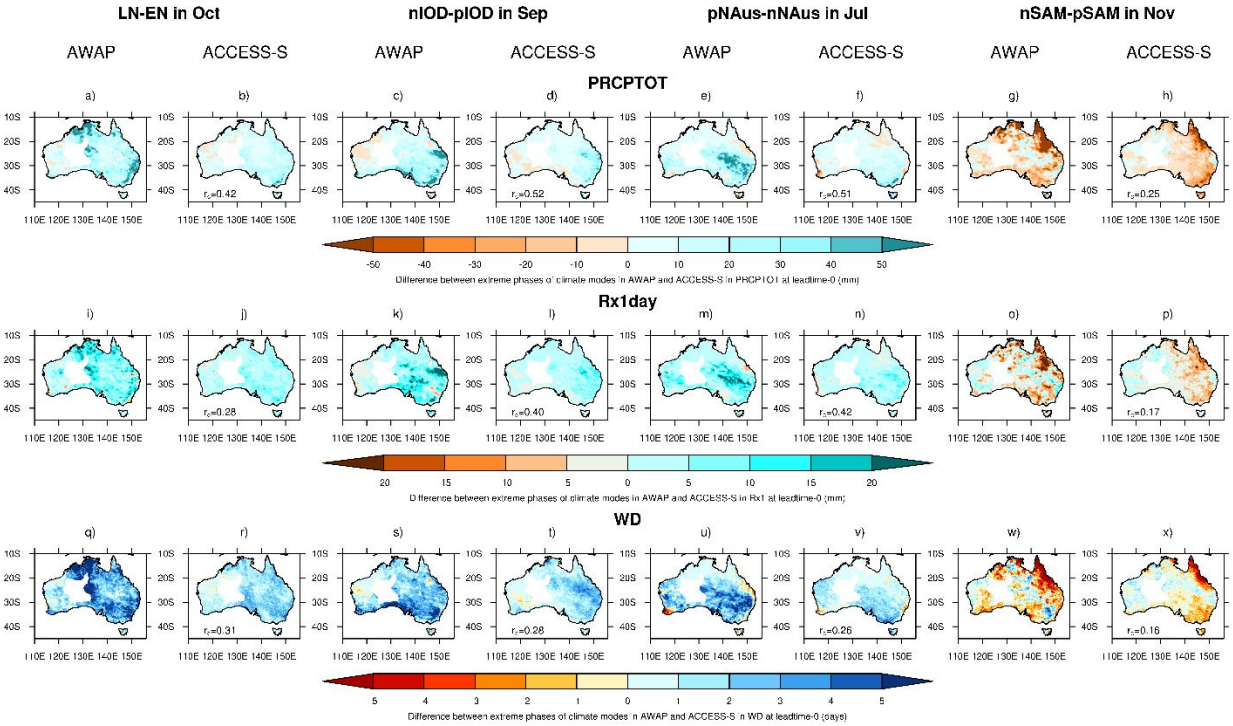

916

917 **Figure 10.** Composite median differences for the five most extreme positive and negative
918 values of each climate mode index observed in the 1990-2012 period (months selected shown
919 in Table 2) for months with strong mean and extreme rainfall relationships to these modes in
920 AWAP and the ACCESS-S1 ensemble median respectively. Differences are shown for a)-h)
921 PRCPTOT, i)-p) Rx1day, and q)-x) WD. The Spearman-rank pattern correlation between the
922 corresponding ACCESS-S1 and AWAP difference maps is shown in each ACCESS-S1 plot.

923

924

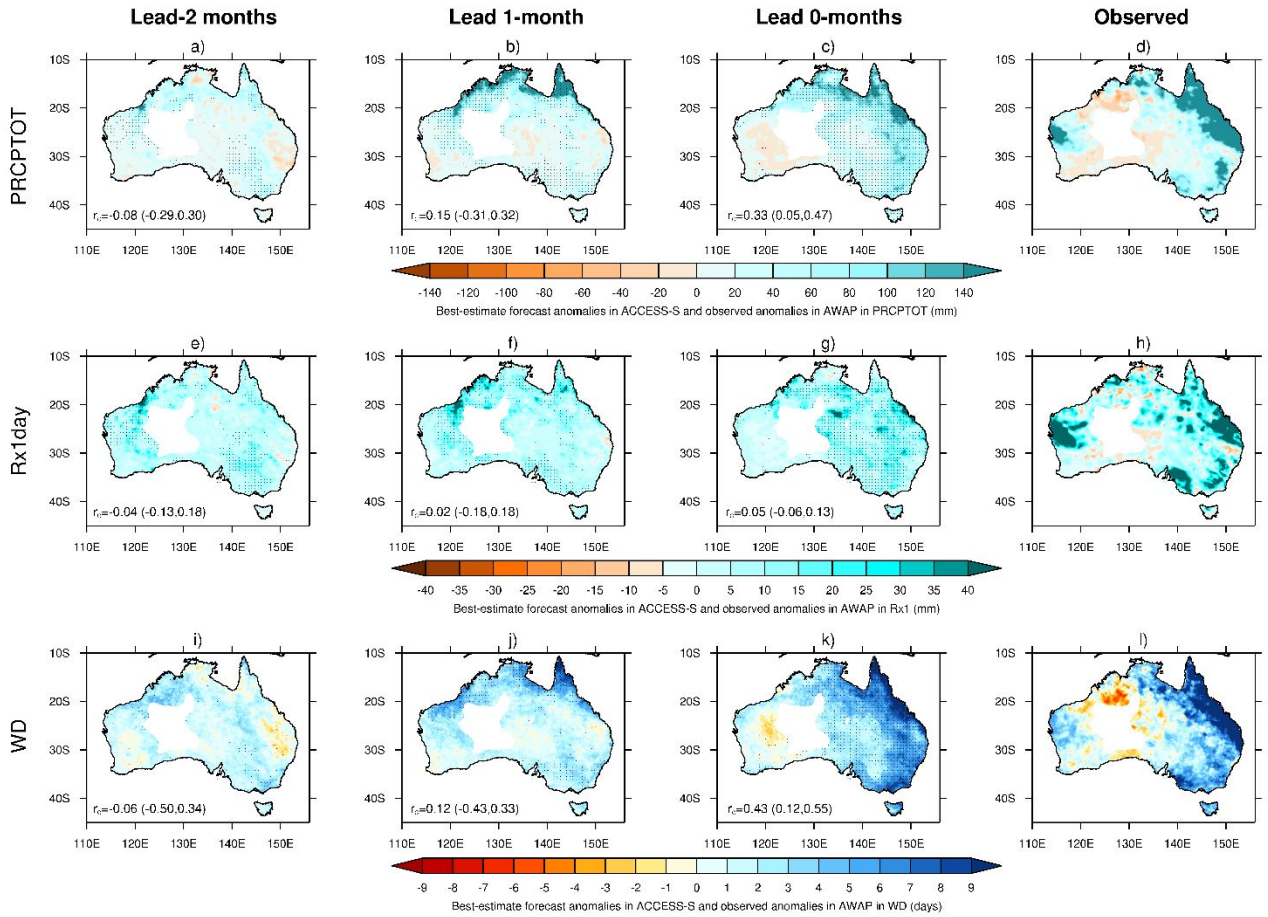

925

926 **Figure 11.** For the extreme wet month of December 2010, the ACCESS-S1 ensemble median
927 anomalies at lead-2, lead-1, and lead-0 are shown with the observed anomalies in a)-d)
928 PRCPTOT, e)-h) Rx1day, and i)-l) WD. Stippling shows at least three-quarters of ensemble
929 members are of the same sign. The median Spearman-rank pattern correlation coefficients
930 between the ACCESS-S1 and observed anomalies are shown in the bottom-left of each plot
931 with the lowest and highest pattern correlation coefficients across the ACCESS-S1 ensemble
932 in parentheses.

933

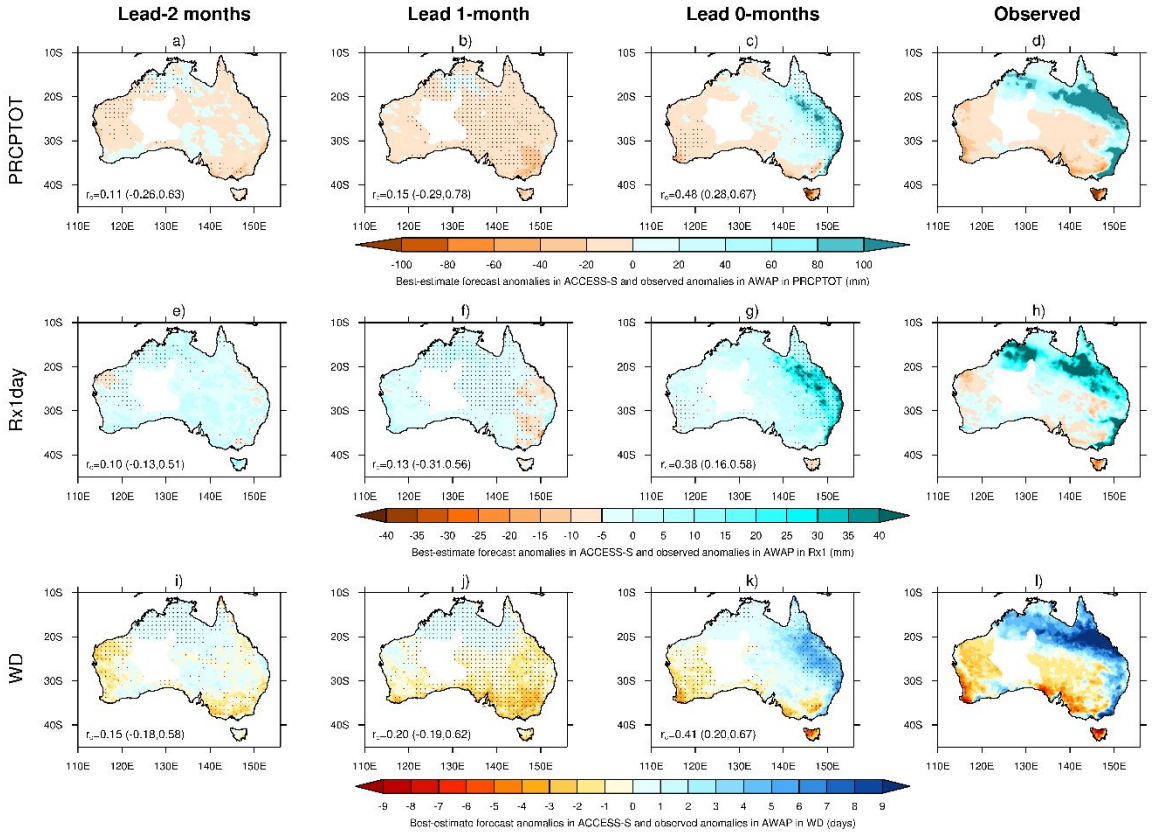

Figure 12. As Figure 11 but for June 2007.

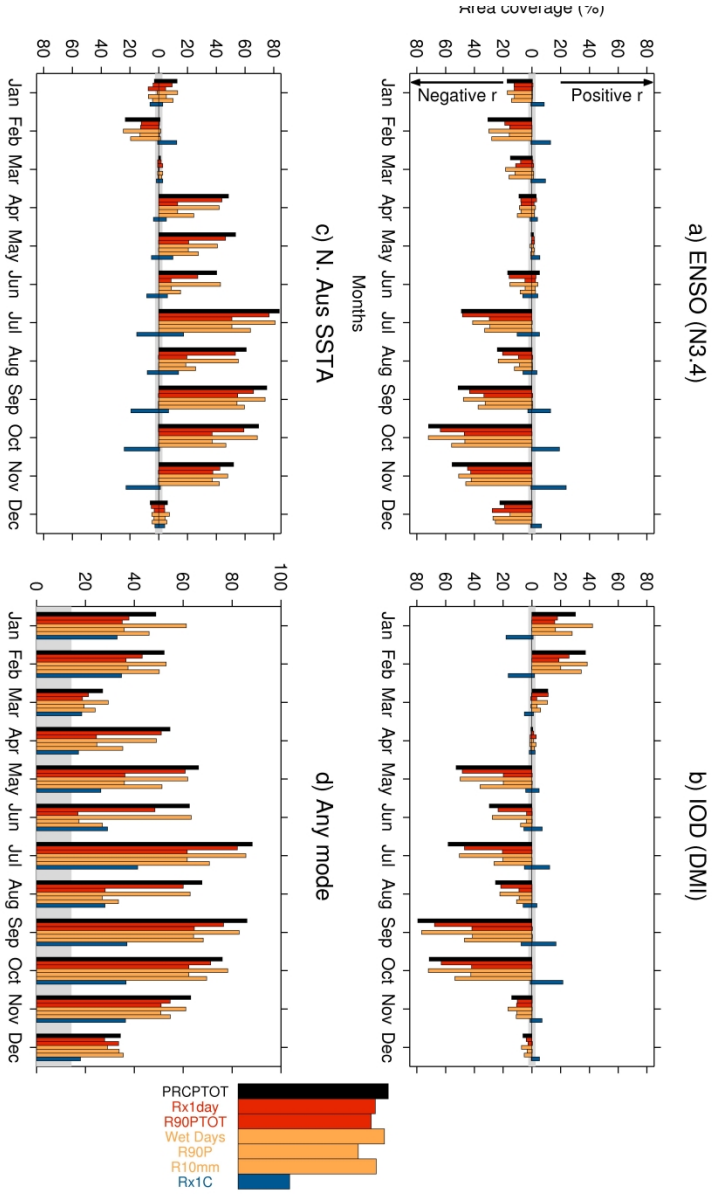

Figure 1. Bar graphs showing the area of Australia with significant concurrent Spearman-rank correlations (p-value < 0.05) between mean and extreme rainfall indices and a) Niño-3.4, b) DMI, c) N. Australian SSTs, and d) any of the three climate modes. Bars in a-c are plotted either above or below the zero line for positive or negative correlations respectively. The grey region indicates the area of significant correlations that might be expected by chance. The legend on the right indicates which bars correspond to which indices with mean rainfall in black, intensity-based indices in red, frequency-based indices in orange and a contribution-based index in blue.

215x279mm (600 x 600 DPI)

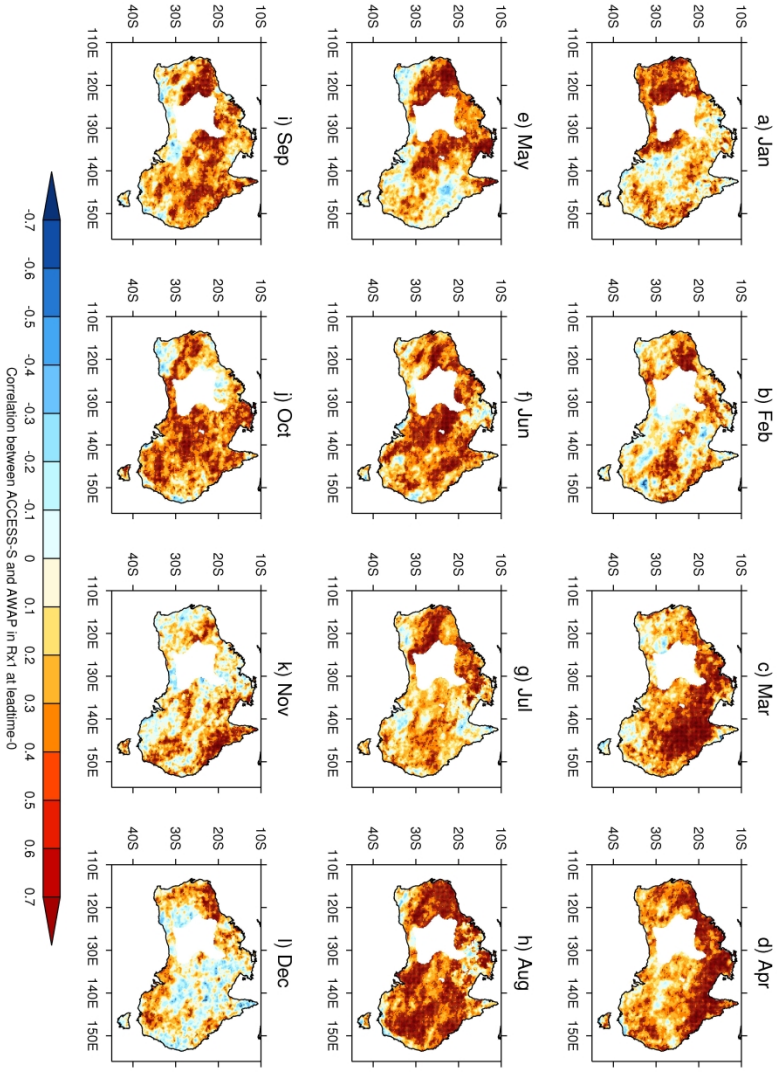

Figure 2. Spearman's rank correlation coefficients in Rx1day between AWAP and the ensemble median ACCESS-S1 value at leadtime-0 for each calendar month from 1990-2012. Stippling indicates correlations significant at the 5% level.

215x279mm (600 x 600 DPI)

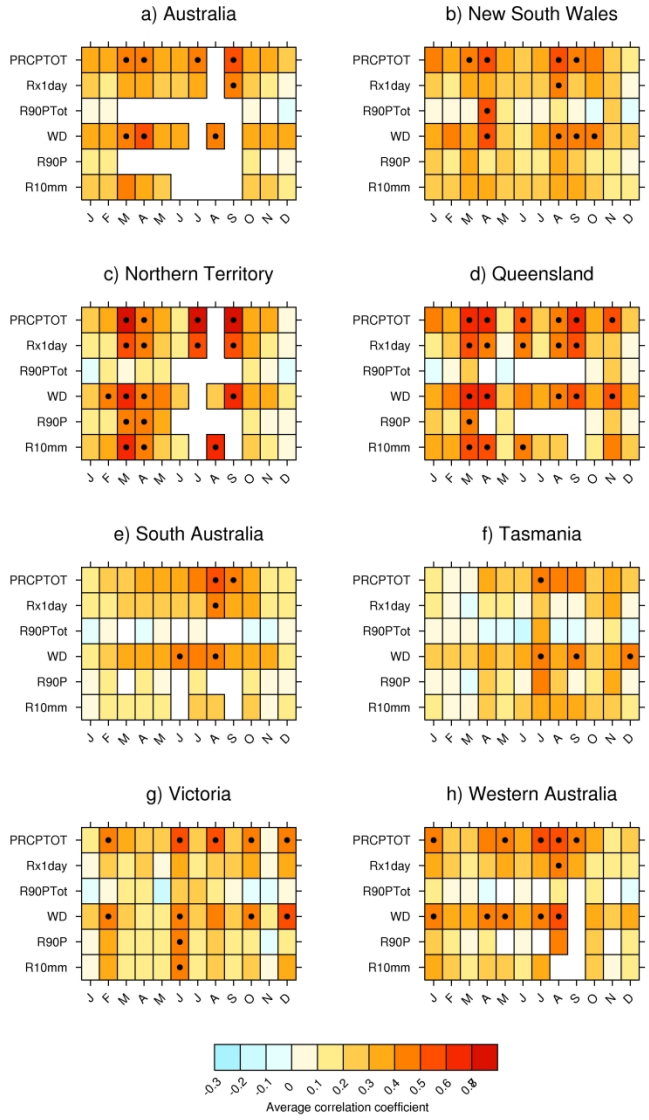

Figure 3. Area-average correlation coefficient matrices for each state of Australia in each calendar month and index at leadtime-0. Black dots indicate correlations significant at the 5% level. These Pearson correlation coefficients are derived by applying the Fisher Z-transform and area-averaging on Z-scores. Grid cells in white show areas where the index has too few non-zero values for reliable correlation calculation.

215x279mm (600 x 600 DPI)

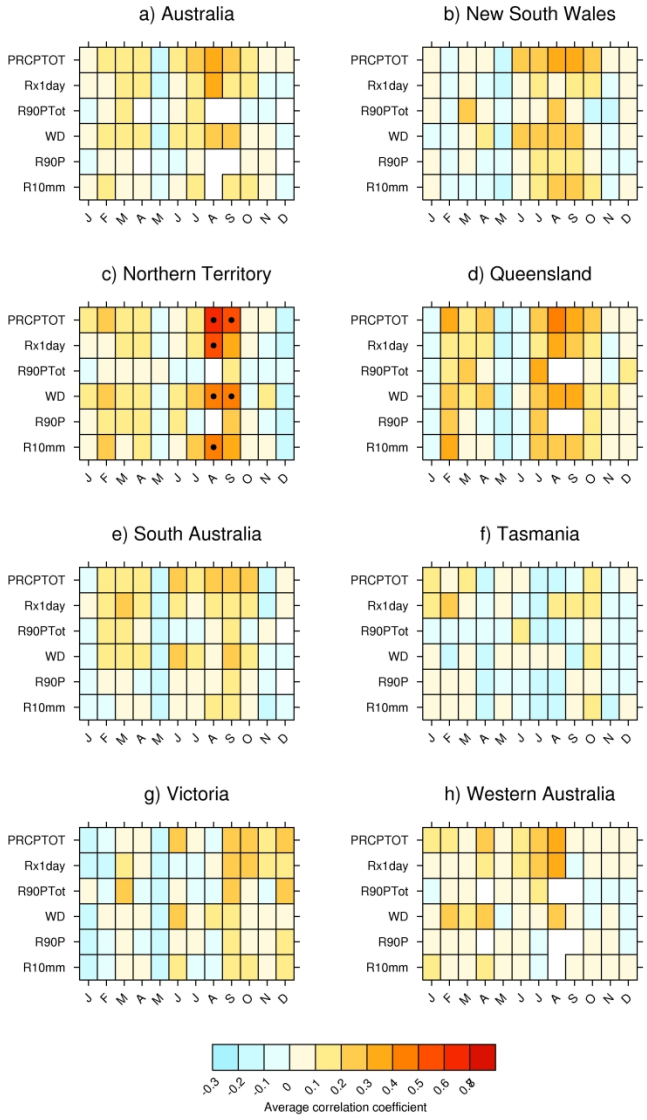

Figure 4. As Figure 3 but for lead-1 month correlation coefficients.

215x279mm (600 x 600 DPI)

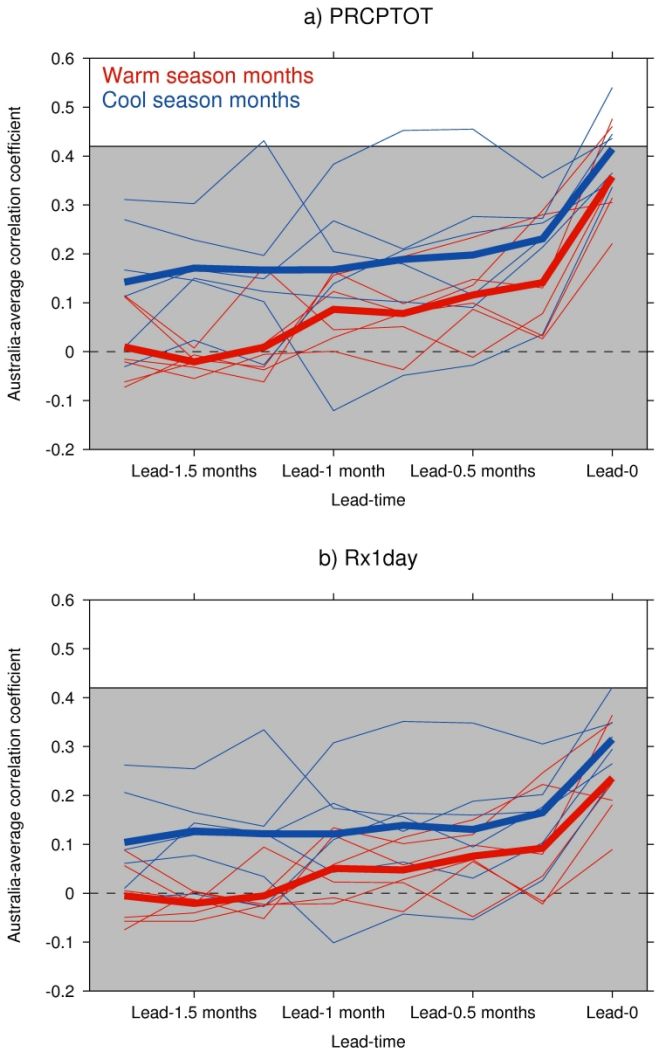

Figure 5. Australian-average correlation coefficients between ACCESS-S and AWAP calculated for each calendar month at every lead-time from 1.75 months in advance to lead-0 for a) PRCPTOT and b) Rx1day. Each thin line represents a different calendar month with months during the warm season marked in red and cool season months in blue. These Pearson correlation coefficients are derived by applying the Fisher Z-transform and area-averaging on Z-scores. The thicker lines represent warm and cool season average correlations at each lead-time computed by averaging the Z-scores from each month at that lead-time. The grey area shows correlations non-significant at the 5% level.

215x279mm (600 x 600 DPI)

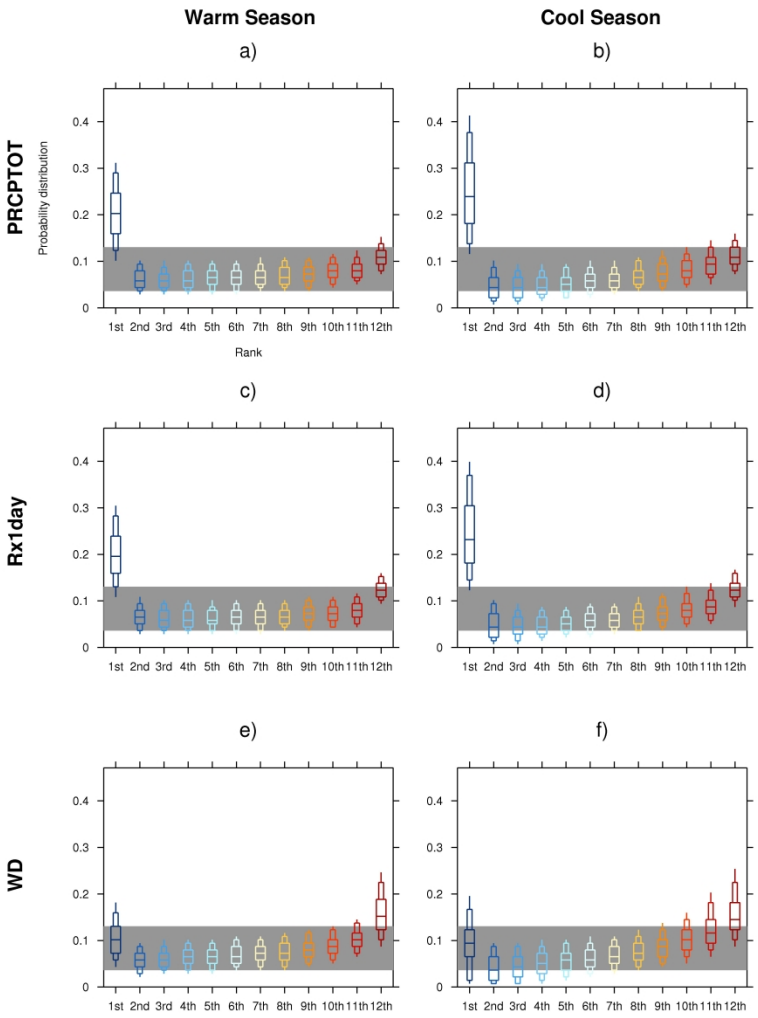

Figure 6. Rank Histograms showing the frequency of ranks of the observed value relative to the ACCESS-S1 ensemble in locations across Australia. The box-plots show the frequency at the median location with the large box representing the interquartile range, the narrower box representing the 10th-90th percentile range, and the whiskers showing the 5th-95th percentile locations. The grey zone represents an estimate of the 95% confidence interval of rank frequencies that could be expected by random chance for the same sample size as is available here.

215x279mm (600 x 600 DPI)

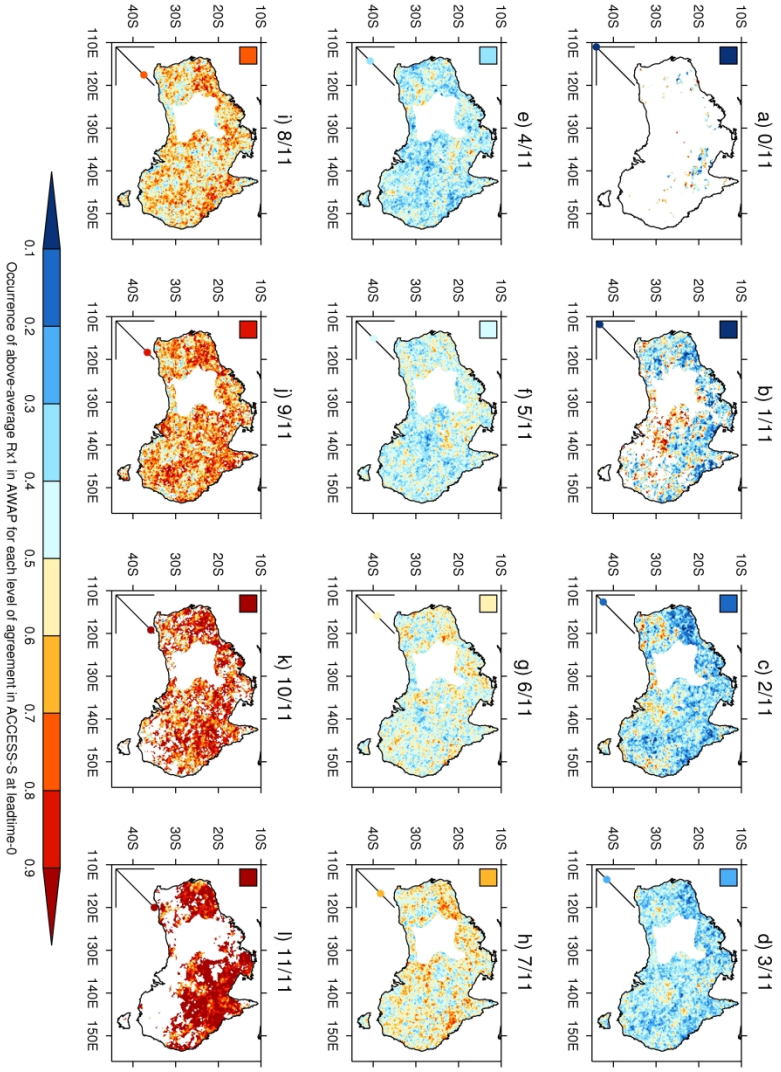

Figure 7. Maps representing the reliability in Rx1day lead-0 predictions in the warm season (Nov-Apr). For cases when each possible fraction of the ACCESS-S1 ensemble is above average, the fraction of corresponding observed values that are above average is shown. The fraction is only shown where there are at least five occurrences where ACCESS-S1 has the fraction of above-average ensemble members considered. The expected colour if ACCESS-S1 is performing well is shown in the top left of each plot and a graphical representation of the point on a reliability diagram being investigated is shown in the bottom-left of each plot.

215x279mm (600 x 600 DPI)

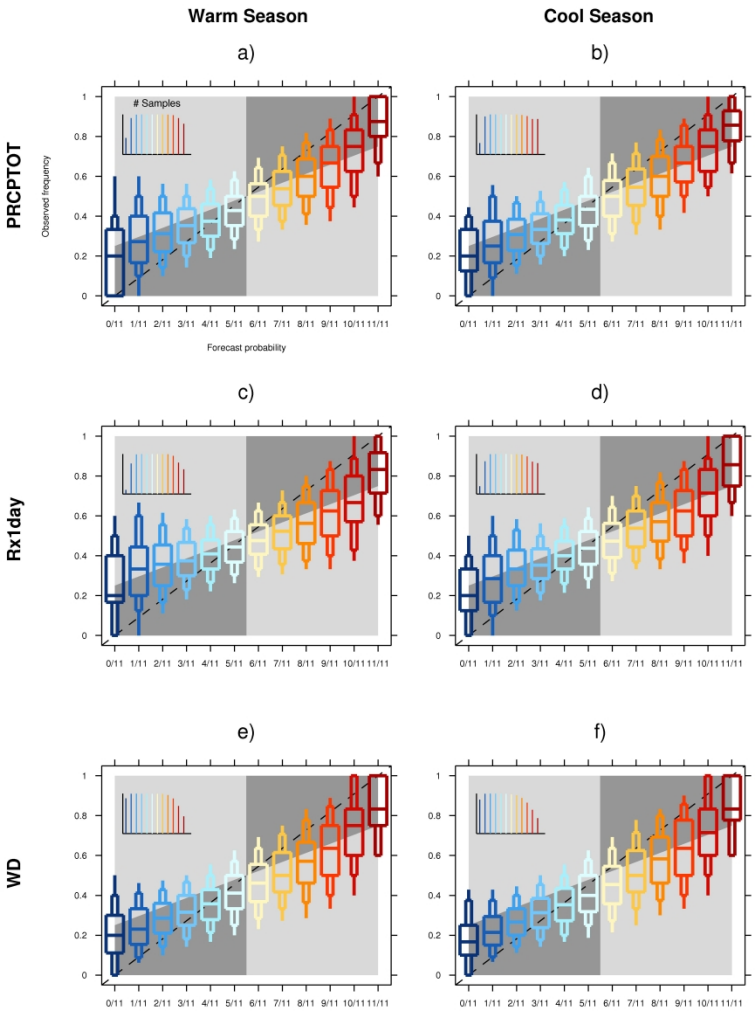

Figure 8. Reliability diagrams aggregating locations across Australia. For each forecast probability of above-average conditions in a), b) PRCPTOT, c), d) Rx1day, and e), f) WD in the warm and cool season respectively, the corresponding observed occurrence is shown with the box-plot representing the range of occurrences across Australia. The box plots use the same percentiles as those in Figure 6. The colours are chosen to match those in Figure 7. Miniature graphs in the top-left of each plot indicate the number of locations contributing to each box-plot as a proportion of the maximum number. The dark grey area shows where a positive contribution to Brier Skill Score is made. The 1:1 line is shown as a dashed black line.

215x279mm (600 x 600 DPI)

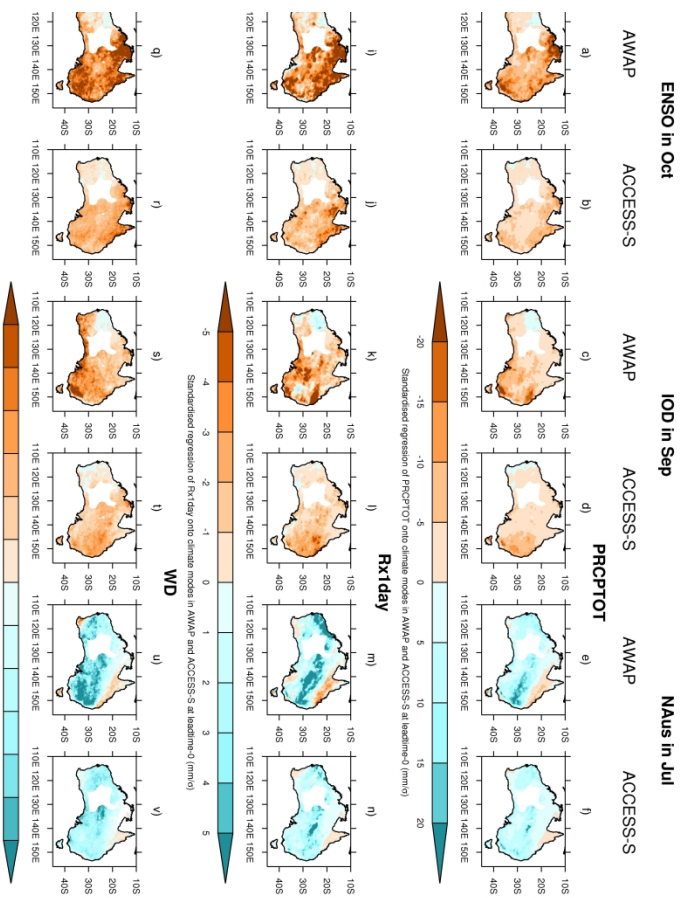

Figure 9. Standardised regression coefficients of mean and extreme rainfall indices onto each climate mode index in the 1990-2012 period for selected months with strong mean and extreme rainfall relationships to these modes in AWAP and the ACCESS-S1 ensemble median respectively. Regression coefficients are shown for a)-h) PRCPTOT, i)-p) Rx1day, and q)-x) WD.

215x279mm (600 x 600 DPI)

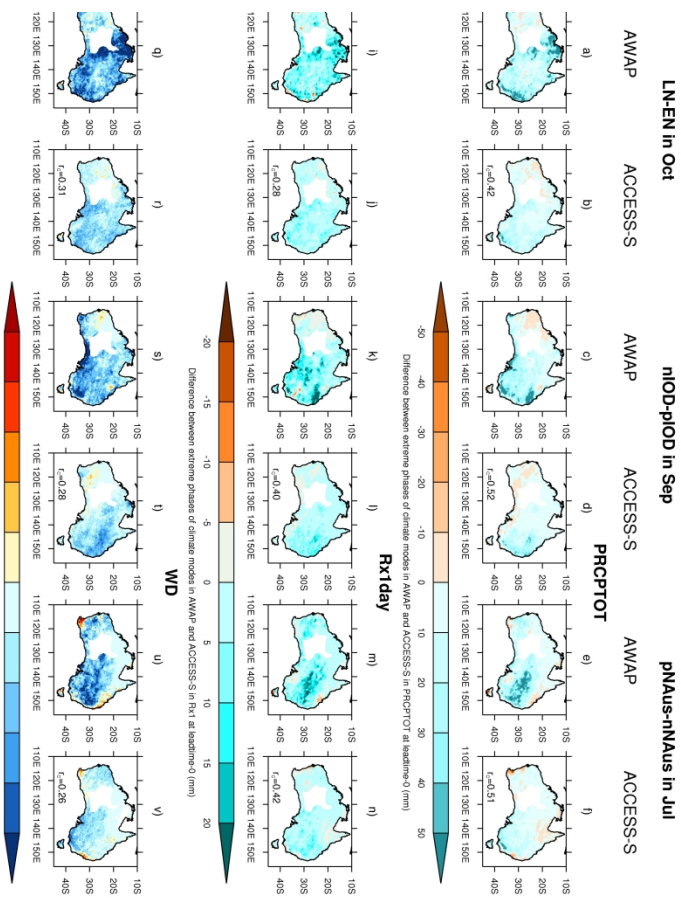

Figure 10. Composite median differences for the five most extreme positive and negative values of each climate mode index observed in the 1990-2012 period (months selected shown in Table 2) for months with strong mean and extreme rainfall relationships to these modes in AWAP and the ACCESS-S1 ensemble median respectively. Differences are shown for a)-h) PRCPTOT, i)-p) Rx1day, and q)-x) WD. The Spearman-rank pattern correlation between the corresponding ACCESS-S1 and AWAP difference maps is shown in each ACCESS-S1 plot.

215x279mm (600 x 600 DPI)

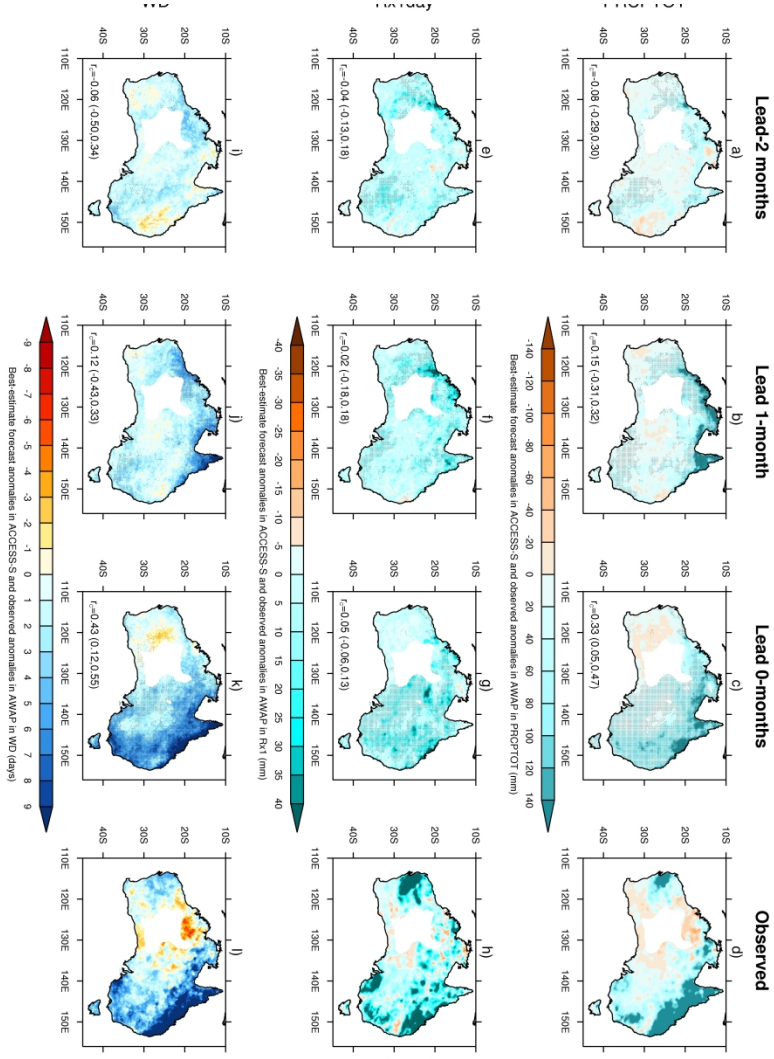

Figure 11. For the extreme wet month of December 2010, the ACCESS-S1 ensemble median anomalies at lead-2, lead-1, and lead-0 are shown with the observed anomalies in a)-d) PRCPTOT, e)-h) Rx1day, and i)-l) WD. Stippling shows at least three-quarters of ensemble members are of the same sign. The median Spearman-rank pattern correlation coefficients between the ACCESS-S1 and observed anomalies are shown in the bottom-left of each plot with the lowest and highest pattern correlation coefficients across the ACCESS-S1 ensemble in parentheses.

215x279mm (600 x 600 DPI)

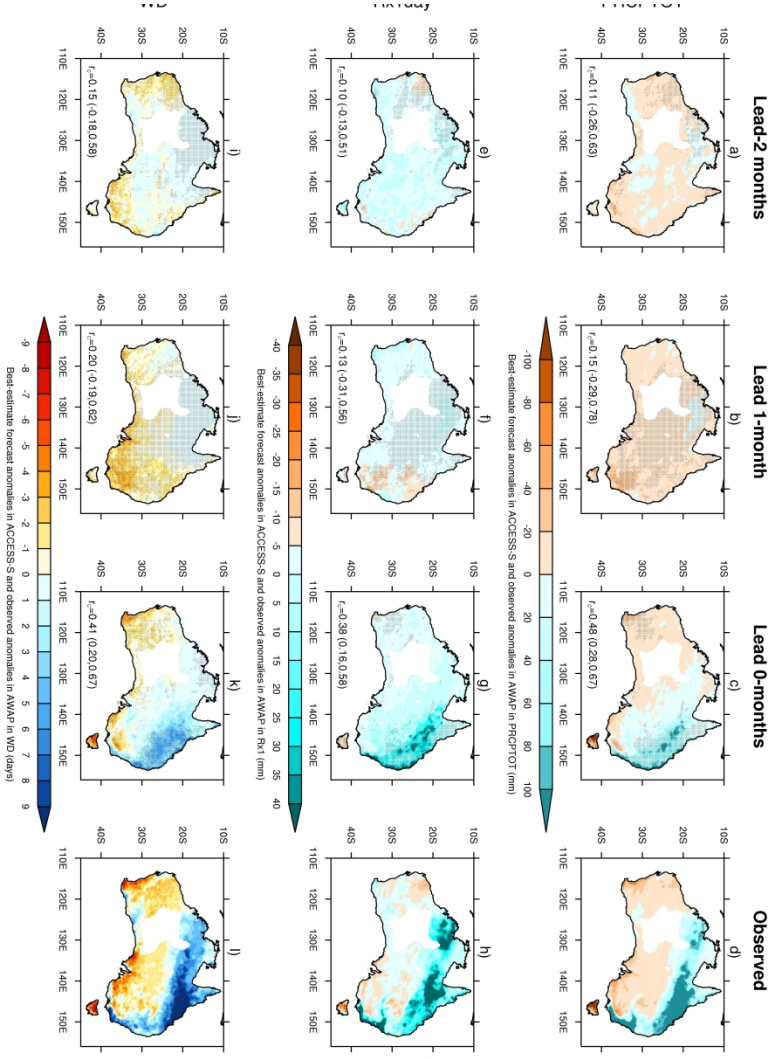

Figure 12. As Figure 11 but for June 2007.

215x279mm (600 x 600 DPI)

Sub-seasonal to seasonal prediction of rainfall extremes in Australia: Graphical Abstract

Andrew D. King[1,*], Debra Hudson[2], Eun-Pa Lim[2], Andrew G. Marshall[3], Harry H. Hendon[2], Todd P. Lane[1], and Oscar Alves[2]

1. School of Earth Sciences and ARC Centre of Excellence for Climate Extremes, University of Melbourne, Melbourne, Victoria, Australia.
2. Bureau of Meteorology, Melbourne, Victoria, Australia.
3. Bureau of Meteorology, Hobart, Tasmania, Australia.

Corresponding Author: Andrew D. King (andrew.king@unimelb.edu.au)

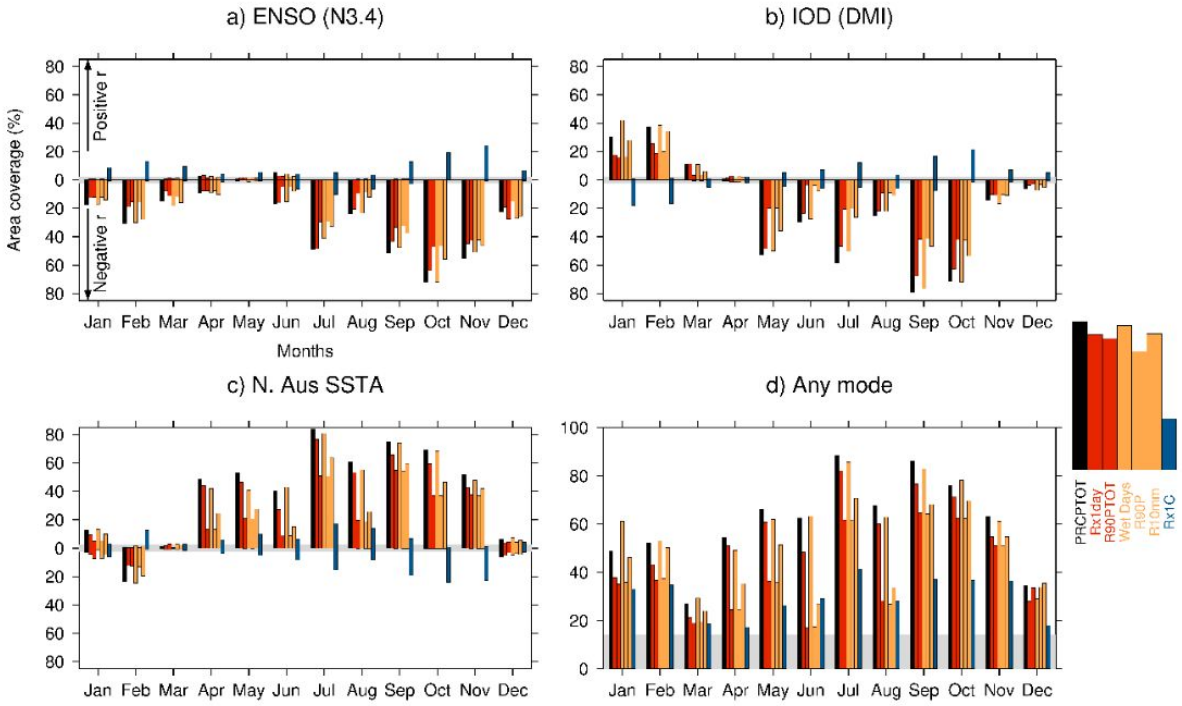

Figure. Bar graphs showing the area of Australia with significant concurrent Spearman-rank correlations (p-value < 0.05) between mean and extreme rainfall indices and a) Niño-3.4, b) DMI, c) N. Australian SSTs, and d) any of the three climate modes. The legend on the right indicates which bars correspond to which indices with mean rainfall in black, intensity-based indices in red, frequency-based indices in orange and a contribution-based index in blue.